

Title: IL-5R α marks nasal polyp IgG4 and IgE-secreting cells in aspirin-exacerbated respiratory disease

List of authors: Kathleen M. Buchheit^{1,3}, Daniel F. Dwyer^{1,3}, Jose Ordovas-Montanes⁵⁻⁷, Howard R. Katz^{1,3}, Erin Lewis, Juying Lai³, Neil Bhattacharyya^{2,4}, Alex K. Shalek⁵⁻⁸, Nora A. Barrett^{1,3}, Joshua A. Boyce^{1,3}, and Tanya M. Laidlaw^{1,3}

¹Department of Medicine, and ²Department of Surgery, Harvard Medical School, Boston, MA; ³Division of Rheumatology, Immunology, and Allergy, and ⁴Division of Otolaryngology, Brigham and Women's Hospital, Boston, MA; ⁵Institute for Medical Engineering and Science (IMES), Department of Chemistry, and Koch Institute for Integrative Cancer Research, MIT, Cambridge, MA, USA, ⁶Broad Institute of MIT and Harvard, Cambridge, MA, USA, ⁷Ragon Institute of MGH, MIT and Harvard, Cambridge, MA, USA, ⁸Harvard-MIT Division of Health Sciences & Technology, Cambridge, MA, USA

Corresponding Author: Tanya Laidlaw, MD

Address: Brigham and Women's Hospital, 60 Fenwood Road, Building of Transformative Medicine, Rm 5002M, Boston, MA 02115

Phone: 617-525-1034

Fax: 617-525-1310

Email: tlaidlaw@bwh.harvard.edu

Conflicts of Interest: A.K. Shalek owns equity in and is an advisor for Honeycomb Biotechnologies, Dot Bio Inc, VL49 Inc, and Dahlia Biosciences. The rest of the authors declare no conflicts of interest. T.M. Laidlaw has received compensation for consulting fees and scientific advisory board membership from Novartis, Regeneron, and Sanofi-Genzyme.

Funding: This work was supported by the National Institutes of Health (NIH grant nos K23HL111113, R01HL128241, T32AI00730), and U19AI070535 and by generous contributions from the Vinik and Kaye Families. AKS was supported by the Searle Scholars Program, the Beckman Young Investigator Program, 5U24AI118672, 2R01HL095791, 2U19AI089992, 1R01HL134539, 1R01AI138546, 1U54CA217377, 1U2CCA23319501, 2RM1HG006193, 2P01AI039671, the Pew-Stewart Scholars, a Sloan Fellowship in Chemistry, and BMGF OPP1139972, OPP1137006, and OPP1116944. J.O.M. is an HHMI Damon Runyon Cancer Research Foundation Fellow (DRG-2274-16).

Abstract:

Background: The cause of nasal polyposis in aspirin-exacerbated respiratory disease (AERD) is unknown. Elevated antibody levels have been associated with disease severity in nasal polyps, but the upstream drivers and cellular mechanisms of local antibody production in AERD remain to be investigated.

Objective: We sought to identify the upstream drivers and phenotypic properties of local antibody-secreting cells in nasal polyps and to understand their clinical relevance in AERD.

Methods: Sinus tissue was obtained from subjects with AERD, aspirin-tolerant chronic rhinosinusitis with nasal polyps (CRSwNP), aspirin-tolerant chronic rhinosinusitis without nasal polyps (CRSsNP), and healthy controls. Tissue antibody levels were quantified via ELISA and immunohistochemistry, and were correlated with clinical markers of disease severity. Tissue cytokine mRNA levels were measured with quantitative PCR (qPCR). Antibody-secreting cells were profiled with a combination of single-cell RNA-sequencing (scRNA-seq), flow cytometry and immunofluorescence.

Results: Tissue IgE and IgG4 were elevated in AERD compared to controls ($p<0.01$ for IgE and $p<0.001$ for IgG4, vs. CRSwNP). Total IgG and IgG4 positively correlated with the number of polyp surgeries per subject ($r=0.48$, $p=0.011$ and $r=0.58$, $p=0.0003$, respectively). Polyp IL-10 mRNA expression was higher in AERD vs. CRSwNP ($p<0.05$), but there were no differences in mRNA expression of type 2 cytokines. ScRNA-seq revealed increased *IL5RA*, *IGHG4*, and *IGHE* in the antibody-associated cells of subjects with AERD compared to CRSwNP. Total plasma cells and IL-5R α^+ plasma cell numbers in the polyp tissue from AERD exceeded those in polyps from CRSwNP ($p=0.0051$ and $p=0.026$, respectively) by flow cytometry. With immunofluorescence, we determined that IL-5R α and IgG4 are co-expressed in antibody-secreting cells in AERD.

Conclusions: Our study identifies unique clusters of antibody-secreting cells in AERD defined by enrichment of transcripts encoding *IL5RA*, *IGHG4* and *IGHE*. We confirm surface expression of IL-5R α on these cells, and identify T cells as a unique transcriptional source of IL-5. Tissue antibody levels are elevated in AERD and correlate with disease severity. Our findings suggest a role for IL-5 in facilitating local antibody production that may drive features of severe sinus disease.

Key Messages:

- IgG4 and IgE levels are markedly increased in nasal polyp tissue from subjects with AERD compared to aspirin-tolerant CRSwNP.
- Tissue IgG4 levels positively correlate with disease recurrence.
- IL-10 mRNA levels are significantly higher in AERD polyp tissue compared to CRSwNP tissue, but differences were not noted for type 2 cytokines or cytokines involved in class switch recombination.
- IL-5RA transcript and protein surface expression is elevated in antibody-secreting cells from subjects with AERD and may play a role in facilitating class switching and/or survival of antibody-secreting cells.

Capsule Summary: Single-cell RNA-sequencing (scRNA-seq) of whole nasal polyp tissue identified increased *IL5RA*, *IGHE*, and *IGHG4* expression in the antibody-secreting cell compartment of subjects with aspirin-exacerbated respiratory disease (AERD) compared to aspirin-tolerant chronic rhinosinusitis with nasal polyps (CRSwNP). IgE and IgG4 levels are elevated in nasal polyp tissue from subjects with AERD compared to CRSwNP and correlate with disease recurrence.

Key Words:

Abbreviations:

AERD	Aspirin-exacerbated respiratory disease
CRSwNP	Chronic rhinosinusitis with nasal polyps
CRSsNP	Chronic rhinosinusitis without nasal polyps
COX	Cyclooxygenase
Ig	Immunoglobulin
IL	Interleukin
LT	Leukotriene
PCA	Principal component analysis
PG	Prostaglandin
scRNA-seq	Single-cell RNA-sequencing
UMAP	Uniform Manifold Approximation and Projection

Introduction:

Nasal polyps are inflammatory outgrowths of sinonasal mucosa that cause nasal obstruction and anosmia, frequently require surgical excision, and are associated with significant medical resource consumption.¹⁻³ Nasal polyps are particularly severe and recurrent in aspirin-exacerbated respiratory disease (AERD), a distinct, adult-onset respiratory syndrome consisting of eosinophilic chronic rhinosinusitis with nasal polyposis (CRSwNP), asthma, and pathognomonic respiratory reactions to cyclooxygenase (COX)-1 inhibitors that involve release of multiple mast cell mediators, including tryptase, leukotriene (LT)C₄ and prostaglandin (PG)D₂.⁴⁻⁶ In patients with AERD, nasal polyps are frequently refractory to standard therapy and recur within two years after surgical excision in 85 percent of patients.⁷ The factors contributing to the severity and recalcitrance of the mucosal pathology in AERD remain largely unknown.

Activated B cells and antibody-secreting cells are present in nasal polyps and locally generate immunoglobulins. Subjects with recurrent nasal polyposis have elevated total nasal polyp IgA, IgG, and IgE levels.⁸⁻¹¹ Potential mechanisms by which local nasal tissue immunoglobulins may contribute to nasal polyp severity include IgE- and free light chain-induced activation of polyp mast cells,¹² IgA-enhanced eosinophil survival,¹³ and IgG-directed local complement activation.¹⁴ IgE antibodies to staphylococcal enterotoxins have been linked to nasal polyp pathogenesis,^{15,16} and a role for auto-antibodies in nasal polyp pathogenesis has been proposed,⁸ but no single antigen has been consistently linked to nasal polyposis in general or to AERD in particular. A previous study reported that patients with AERD have elevated serum IgG4 and slightly depressed serum IgG1 as compared to healthy controls, independent of corticosteroid exposure or IgE levels.¹⁷ More recently, IgG4 was identified in nasal polyp tissue from subjects with CRS and AERD and was correlated with a poor post-operative course.¹⁸ This suggests a possible role for IgG4 in sinus disease persistence by as yet unidentified mechanisms.

Nasal polyp tissue contains a variety of cytokines that may drive the B cell pro-inflammatory response.¹⁹ Type 2 cytokines, including IL-4, IL-5, IL-13, TSLP, and IL-33, as well as IL-10, are abundant in the eosinophilic nasal polyps in AERD.^{6,20,21} Some of these type 2 cytokines have been shown to influence B cell differentiation, activation and class switching, and can drive immunoglobulin production in other settings.^{22,23} In the current study, we use massively parallel single-cell RNA-sequencing (scRNA-seq) and flow cytometry to identify unique antibody-secreting cell states in nasal polyps from patients with AERD. These antibody-secreting cells express *IL5RA*, encoding for the IL-5 receptor alpha subunit (IL-5R α), along with *IGHG4* and *IGHE*, encoding for the IgG4 and IgE heavy chains. Both IgE and IgG4 concentrations are selectively elevated in the nasal polyp tissue of subjects with AERD. Furthermore, those elevated antibody levels correlate with the severity and recurrence of the sinus disease. We suspect that the increased IgE may be pathogenic and driven in part by the effect of local T cell derived IL-5 on antibody-secreting cells in the nasal polyp tissue, and that the increased IgG4 may be a compensatory mechanism reflecting the additional influence of IL-10 from myeloid cells on local class switching. Moreover, in addition to its established role in controlling tissue eosinophilia, IL-5 may also drive pathogenic immunoglobulin production, and may be amenable to modification with IL-5-neutralizing biologic therapies.

Methods:

Patient characterization

Subjects between the ages of 18 and 75 years were recruited from the Brigham and Women's Hospital (Boston, MA) Allergy and Immunology clinics and Otolaryngology clinics

between May 2013 and June 2018 (**Table 1**). The local Institutional Review Board approved the study and all subjects provided written informed consent. Ethmoid sinus tissue was collected at the time of elective endoscopic sinus surgery from patients with physician-diagnosed AERD, and aspirin-tolerant CRS with and without nasal polyps with the diagnosis made based on established guidelines.²⁴ Healthy control patients were undergoing sinus surgery to correct anatomic abnormalities by removal of concha bullosa. Patients were suspected of having AERD if they had asthma, nasal polyposis, and a history of respiratory reaction on ingestion of a COX-1 inhibitor, with diagnosis later confirmed in all subjects via a physician-observed graded oral challenge to aspirin. Subjects with known cystic fibrosis, allergic fungal rhinosinusitis and unilateral polyps were excluded from the study.

Polyp procurement and tissue specimen preparation

Nasal tissue was excised at the time of surgery; one tissue segment was immediately preserved in RNAlater (Qiagen, Valencia, CA) for RNA extraction, and the remaining tissue was placed in RPMI (Corning, Corning, NY) with 10% fetal bovine serum (ThermoFisher, Waltham, MA) and 1 U/mL penicillin-streptomycin for transport to the laboratory on ice. Within 2 hours of surgery, the tissue was removed from RPMI and divided into segments. One segment was transferred into Cell Lytic M Cell Lysis Reagent (Sigma-Aldrich, St Louis, MO) with 2% protease inhibitor (Roche, Indianapolis, IN) for protein extraction, and the tissue was homogenized with a gentleMACS Dissociator (Miltenyi Biotec, San Diego, CA). Supernatants were stored at -80°C. One segment was fixed in 4% paraformaldehyde, embedded in paraffin, and kept at -80°C until sectioning. For some patients, a tissue segment was also digested into a single-cell suspension for flow cytometric studies as described below.

Tissue Digestion

Single-cell suspensions from surgical specimens were obtained using a modified version of a previously published protocol.²⁵ Surgical specimens were collected into 30 mL of cold RPMI with 10% fetal bovine serum and 1 U/mL penicillin-streptomycin. Specimens were finely minced between two scalpel blades and incubated for 15 minutes at 37°C with 600 U/mL collagenase IV (Worthington, Lakewood, NJ) and 20 ug/mL DNase 1 (Roche, Indianapolis, IN) in RPMI with 10% fetal bovine serum. After 15 minutes, samples were triturated five times using a syringe with a 16G needle and incubated for another 15 minutes. At the conclusion of the second digest period, samples were triturated an additional five times using a syringe with a 16G needle. Samples were typically fully dissociated at this step and were filtered through a 70 µm cell strainer and spun down at 500G for 10 minutes followed a rinse with ice-cold Ca/Mg free PBS (ThermoFisher, Waltham MA) to 30 mL total volume. Red blood cells were lysed using ACK buffer (ThermoFisher) for three minutes on ice to remove red blood cells, even if no red blood cell contamination was visibly seen in order to maintain consistency across patient groups. Single-cell suspensions were cryopreserved in CryoStor CS10 (Sigma) for batched flow cytometric analyses.

Quantitative PCR

RNA was extracted from the whole nasal tissue specimens with Tri Reagent (Qiagen) and converted to cDNA by using the RT² First Strand Kit (Qiagen). Expression of *IL4*, *IL5*, *IL6*, *IL7*, *IL10*, *IL13*, *IL21*, *IL23*, *TGFBI*, *IFNA1*, *CXCL12*, *CXCL13*, *PRDM1*, and *TNFSF13B* transcripts was examined using RT2 SYBR Green qPCR Master Mix (Qiagen), and normalized to

glyceraldehyde-3-phosphate dehydrogenase (*GAPDH*; all primers from Qiagen).

Immuno globulin quantification

Protein lysate supernatants from sinonasal tissue were collected as described above. Total IgG, IgA, IgE, and IgG1, IgG2, IgG3, and IgG4 ELISAs (eBioscience, San Diego CA) were performed according to the manufacturer's instructions. Total tissue protein levels were measured with the Pierce® BCA Protein Assay kit (Thermo Scientific). Tissue immunoglobulin levels were normalized to total protein levels.

Immunohistochemistry and Immunofluorescence

Tissue segments were fixed in 4% paraformaldehyde, embedded in paraffin, and 5 µm sections were prepared and incubated with a mouse anti-human IgG4 mAb (clone MRQ-44; Sigma) or isotype control. For immunohistochemistry, staining was developed with the EnVision System-HRP for mouse primary antibodies (Dako, Carpinteria, CA). Sections were counterstained with hematoxylin, Gill no. 2. For quantification of IgG4⁺ cells, numbers of IgG4-positive cells in photomicrographs encompassing at least 3 high power fields of subepithelial tissue were counted and expressed per high power field. For immunofluorescence, sections were blocked with 10% donkey serum, then were incubated with both mouse anti-IgG4 and a rabbit polyclonal anti-human IL-5Ra Ab (Sigma PA5-25159) or rabbit IgG in the first step, and staining was developed with AF 594 F(ab')₂, donkey anti-mouse IgG and AF 488 F(ab')₂, donkey anti-rabbit IgG.

scRNA-Seq Analysis

Ethmoid scRNA-seq data was obtained from a previously published study,²⁶ available from the dbGaP database under dbGaP accession 30434. The UMI-collapsed cells-by-genes matrix was input into Seurat,²⁷ and clustering was conducted as previously described.²⁶ Iterative clustering was conducted on the previously-defined Plasma cell cluster, consisting of 2,520 cells across 12 patient samples. Briefly, a list of the 1,902 most variable genes among these cells was generated by including genes with an average normalized and scaled expression value greater than 0.22 and with a dispersion (variance/mean) of between 0.22 and 7. Principal component analysis (PCA) was performed over this list of variable genes with the addition of all immunoglobulin isotype heavy chain constant regions and first 8 principal components (PCs) were selected for further analysis based on visual identification of the “elbow” in a plot of the percent variance explained per PC. Clusters were determined using FindClusters (utilizing a shared nearest neighbor (SNN) modularity optimization based clustering algorithm) on the first 8 principal components with a resolution of 0.7. Cells were then graphically displayed using Uniform Manifold Approximation and Projection (UMAP) with a minimum distance of 0.75.

To determine cytokine sources within AERD polyps, the 4,276 cells collected from AERD patient polyps were iteratively clustered in the following fashion. A list of the 1,902 most variable genes was generated using the criteria outlined above. After performing PCA, the first 15 PCs were used for clustering and UMAP display following visual inspection of the principal component elbow graph and determining the inflection point. We note that this number of PCs separated all previously-identified cell types. Cellular identities were retained from previous analysis of this dataset.²⁶ Sub-analysis of the 282 myeloid cells was conducted on the 2,324 most variable genes, determined as previously mentioned. The first 5 PCs were utilized for clustering and UMAP following visual inspection of the PC elbow plot, and clustering was performed with a resolution of 0.6. Sub-analysis of the 224 T lymphocytes was

conducted on the 2,587 most variable genes, determined as previously mentioned. The first 6 PCs were utilized for clustering and UMAP following visual inspection of the PC elbow plot, and clustering was performed with a resolution of 1.0.

Flow cytometry

Cells from the digested nasal polyp single cell suspension were stained with mAbs against CD45, CD3, CD4, CD27, CD38, CD138 (eBiosciences), IL-5R α and CD20 (BD Biosciences, Franklin Lakes NJ) to identify plasma cells/plasmablasts, B cells, and expression of the IL-5R α . Plasma cells were defined as CD45 $^+$ /CD3 $^-$ /CD20 $^-$ /CD27 $^+$ /CD38 $^+$ /CD138 $^+$ and B cells were defined as CD45 $^+$ /CD3 $^-$ /CD20 $^+$.

Statistical analysis

Data are presented as individual points plus standard error (SEM), unless otherwise specified. For the immunoglobulin analyses, comparisons were performed with the Kruskal-Wallis one-way ANOVA due to non-Gaussian distribution of the data. Binary comparisons were carried out with the Mann-Whitney test. Significance was defined as a two-tailed *P*-value of less than 0.05. For the whole polyp mRNA cytokine analyses, comparisons were performed with an unpaired, 2-tailed *t*-test. For the IL-5R α surface expression analysis, comparisons were carried out with the Mann-Whitney test. Linear dependence was measured with the Spearman correlation coefficient. Statistical analyses were performed using GraphPad Prism v7.0a (GraphPad Prism, La Jolla, CA).

For scRNA-seq, data was analyzed with Seurat 2.3.4²⁷ implemented in RStudio. Disease-of-origin enrichment in clusters was determined in Prism using the binomial test. All violin plots, which we elected to use due to zero inflation in single-cell data, contain at minimum 292 individual data points in any one patient group. Violins were generated through default code implemented in Seurat. Statistical enrichment for genes within clusters and disease states was determined using the Tobit test for differential gene analysis.²⁸ For scores in single-cell data, we report effect sizes in addition to statistical significance as an additional metric for the magnitude of the effect observed. The calculation was performed as Cohen's *d* where: effect size *d* = (Mean1-Mean2)/(S.D. pooled).

Results:

Study population and demographics

There were no statistically significant differences in age or sex between subjects with CRSwNP, CRSsNP, and AERD. Healthy control subjects with surgical excision of concha bullosae were all female (5 of 5 subjects). The lifetime number of polyp surgeries was significantly higher (*P* < 0.001) and the time to polyp recurrence was significantly shorter (*P* < 0.0001) in AERD subjects compared to aspirin-tolerant CRSwNP (**Table I**). All patients with AERD had physician-diagnosed asthma and their AERD diagnosis had been confirmed with an oral aspirin challenge, and 7 of 28 aspirin-tolerant CRSwNP patients had a diagnosis of asthma.

Nasal polyp immunoglobulin levels are elevated in AERD

Polyp tissue lysates from subjects with AERD contained significantly higher concentrations of IgA, IgG, and IgE compared to sinonasal tissue from healthy controls and CRSsNP (**Figure 1 A – C**). Polyp IgE concentrations were higher in the AERD samples than in those from CRSwNP samples (*P* < 0.01), and IgA and IgG levels tended to be higher as well (**Figure 1 A – C**). In subjects with nasal polyposis, there was a correlation between immunoglobulin levels and total lifetime number of sinus surgeries, which was used as a

surrogate for disease severity (**Figure 1 D – F**). Total immunoglobulin levels did not correlate with subject age (data not shown). There was no correlation between serum IgE and polyp IgE levels in the samples from the 22 patients for whom both serum and polyp IgE levels were available (data not shown).

To identify the isotypes responsible for the increased IgG levels in polyps from subjects with AERD, we measured specific isotypes by ELISA. Nasal polyp IgG4 protein levels were more than 6-fold higher in subjects with AERD than with CRSwNP ($P < 0.0001$), 43-fold higher in AERD compared to CRSsNP ($P < 0.001$) and close to 300-fold higher in AERD compared to healthy controls ($P < 0.0001$) (**Figure 2A**). Furthermore, nasal polyp IgG4 levels correlated with total lifetime number of sinus surgeries ($P < 0.01$) (**Figure 2B**). IgG4 as a percent of total IgG was significantly higher in subjects with AERD as compared to aspirin tolerant CRSwNP ($P = 0.005$) (**Figure S1**), but there was no difference among the four phenotypic groups in their levels of IgG1, IgG2, and IgG3 as a percentage of total IgG (data not shown). Notably, nasal polyp IgG4 levels did not correlate with IgE levels in the same samples (data not shown).

To further confirm our findings, we immuno histochemically evaluated nasal polyp tissue for IgG4⁺ antibody-associated cells. We found that subjects with AERD had over 5-fold more IgG4⁺ cells compared to subjects with CRSwNP (**Figure 2C-E**). The IgG4⁺ cells did not appear to organize into lymphoid aggregates.

Type 2 cytokine and B cell function-related mRNA expression in nasal polyp subsets

To determine the factors driving local IgG4 production in the nasal polyp tissue of subjects with AERD, we used qPCR to measure mRNA for a number of cytokines potentially involved in immunoglobulin production and class switch recombination in the nasal polyp tissue of subjects with AERD and CRSwNP. There was significantly more *IL10* mRNA present in the whole nasal polyp tissue of subjects with AERD compared to CRSwNP ($P = 0.034$) (**Table 2**), but no differences in type 2 cytokine mRNA levels measured, including *IL4* and *IL13*, or in other cytokines or growth factors relevant to B cell function, including *IL6* and *TGFBI* (**Table 2**). We could not detect *IL21* transcript in a sufficient number of samples to make a comparison between groups (data not shown). IL-5 protein was below the limit of ELISA detection in most of our samples (data not shown).

ScRNA-seq identifies a transcriptionally distinct antibody-producing cell cluster unique to AERD

To extend our primary observations and identify the cellular sources of class switch-associated cytokines in an unbiased fashion, we utilized a previously-generated scRNA-Seq dataset of surgically-resected and dissociated nasal polyp tissue from a cohort of three subjects with AERD, three subjects with aspirin-tolerant CRSwNP, and five subjects with CRSsNP, specifically focusing on the previously-identified antibody-secreting cell clusters.²⁶ Iterative clustering of these populations yielded 9 clusters (**Figure 3A**), all of which contained cells derived from at least eight donors and all three disease states (**Figure S2**). The majority of cluster-defining genes encoded immunoglobulin components (**Supplementary Table E1**). As previously observed,²⁶ kappa and lambda light chain usage underlies a major division between clusters (**Figure S3A**). Little *IGHM* or *IGHD* expression was observed (**Figure S3B**), while robust expression of IgA and IgG isotype regions informs the remaining clusters, indicating that the majority of antibody-secreting cells detected were class-switched (**Figure S2C**).

Interestingly, clusters 2, 3, 4, 6, and 7 showed significant enrichment for cells derived from AERD patients (**Figure 3B**).

To understand the disease-specific differences underlying our clustering, we specifically compared transcript expression between AERD, CRSwNP and CRSsNP-derived antibody-secreting cells (**Supplementary Table E2**). *IGHG4*, encoding the IgG4 constant region, was significantly increased in AERD relative to CRSwNP and CRSsNP (**Figure 3C, Figure S3C**), confirming a local source for the increased protein levels (**Fig. 2A**). We similarly saw enriched expression for *IGHE*, encoding the IgE constant region (**Figure 3C, Figure S3D**).

To gain additional insights into potential mechanisms regulating these AERD-enriched antibody-secreting cell clusters, we further analyzed the underlying gene lists to look for unique cell-surface receptor expression. Despite not identifying significant differences in *IL5* mRNA levels in bulk tissue, we found that all AERD-derived antibody-secreting cells were significantly enriched for *IL5RA* (**Figure 3C, Figure S3E**), encoding IL-5R α , and further observed that this was the sole enriched cytokine receptor (**Supplemental Table E2**).

To understand the contribution of different cell types to cytokine production in AERD, we utilized our previously-generated scRNA-seq dataset of dissociated nasal polyp cells from subjects with AERD. ScRNA-seq of all polyp cells revealed the cellular identity of respiratory epithelial, stromal and immune cell types in the nasal polyp tissue (**Figure S4**). We examined the transcripts of each cell type to identify the potential cell-of-origin for type 2 cytokines possibly involved in class switching to IgE and IgG4 in AERD. Myeloid cells were the dominant source of *IL10*, with IL-10 expression specifically mapping to the previously identified *S100A8*-expressing inflammatory DC-3 and *C1Q*-expressing macrophages²⁶ within the myeloid cluster (**Figure S4 B**). IL-5 expression was restricted to the T cell cluster, and sub-analysis indicated that these T cells co-expressed *IL13* and *HPGDS*, suggestive of the recently identified Th2A cell²⁹ (**Figure S4 C**).

Surface expression of IL-5R α antibody secreting cells from nasal polyps

To further evaluate differences in antibody-secreting cells between subjects with AERD and CRSwNP, we examined plasma cells in the nasal polyp single cell suspensions from subjects with AERD and CRSwNP. We flow cytometrically quantified plasma cells as CD45 $^{+}$ /CD3 $^{-}$ /CD20 $^{-}$ /CD27 $^{+}$ /CD38 $^{+}$ /CD138 $^{+}$ and found that subjects with AERD have significantly higher numbers of plasma cells within their nasal polyps compared to tissue from subjects with aspirin-tolerant CRSwNP ($P = 0.0051$) (**Figure 4A**). There was no significant difference in the percentage of CD45 $^{+}$ cells that were B cells in subjects with AERD ($5.5 \pm 1.8\%$) vs. CRSwNP ($3.5 \pm 0.7\%$, $P = 0.35$). The plasma cells in nasal polyps from subjects with AERD also had greater surface expression of IL-5R α compared to tissue from subjects with aspirin-tolerant CRSwNP ($P = 0.026$) (**Figure 4B, C**). Using immunofluorescence, we examined nasal polyp tissue from 3 patients with AERD and identified co-localization of IL-5R α and IgG4 in antibody-secreting cells (**Figure 4D**, representative sample).

Discussion:

Neither the regulatory factors nor the direct consequences of local immunoglobulin production in nasal polyp tissue are known. Furthermore, differences in immunoglobulin production levels between subjects with aspirin-tolerant CRSwNP and AERD had not previously been recognized. Due to the potential importance of IgE and IgG4 in AERD pathogenesis and the potential for additional antibody-driven effector mechanisms, we sought to characterize local

immunoglobulin production in nasal polyp tissue in subjects with AERD and identify factors that influence the relevant antibody-secreting cells.

We tested whole nasal polyp extracts from patients with AERD, aspirin-tolerant CRSwNP, and controls with CRSsNP and concha bullosa tissue (as a surrogate healthy control tissue) for concentrations of discrete antibody isotypes. As anticipated, polyps contained all antibody isotypes at higher concentrations than in controls, and total polyp IgG ($r=0.48$, $P=0.011$) and IgG4 ($r=0.58$, $P=0.0003$) correlated with lifetime numbers of polyp surgeries, with a weak IgE correlation as well ($r=0.35$, $P=0.052$) (**Figure 1E-F and Figure 2 B**). While all antibody levels tended to be higher in the polyps from AERD subjects than those from CRSwNP, the differences between these two groups in total IgE (**Figure 1C**) and IgG4 (**Figure 2**) were remarkable. Moreover, polyp IgE levels did not correlate with serum IgE from the same subjects (data not shown), suggesting that IgE was synthesized locally. IgE-producing cells are notoriously difficult to detect due to very low receptor density compared with other isotypes, and their ephemeral nature in memory B cell pool of blood and secondary lymphoid organs.³⁰ However, IgG4⁺ cells were readily detectable in the AERD polyps, and far more numerous than in the aspirin-tolerant control polyps, and rare IgE-expressing cells could be observed through scRNA-seq analysis (**Figures 2C-E, 3, S3**). These observations support mechanisms that specifically regulate the local productions of IgE and IgG4 in nasal polyps, and that strongly differentiate AERD from CRSwNP. It is suspected that local tissue mast cell activation contributes to nasal tissue inflammation in AERD, though the underlying mechanisms that lead to chronic mast cell activation in the tissue have not been elucidated. Although many subjects with AERD lack classic atopy,³¹ they do tend to have elevated systemic IgE levels.³¹ A recent study reported that treatment with omalizumab, a monoclonal antibody against IgE, improved sinonasal symptoms in patients with AERD and also decreased urinary PGD₂ metabolite and leukotriene E₄ levels, both of which are likely derived from mast cells, by ~90%.³² Therefore, the elevated levels of IgE (**Figure 1C**) we have found in the local nasal tissue could be instrumental to the mast cell activation within the nasal polyp tissue in AERD. However, our data suggests that the IgG4 production more strongly contributes to the severity and aggressive regrowth of nasal polyps observed in these patients.

Whereas locally-generated IgE may permit mast cells, basophils, and other FcεRI-bearing effector cells to respond to cryptic or microbial antigens, the pathophysiologic significance of IgG4 is not clear. Like IgE production, IgG4 production by B cells is regulated by IL-4/IL-13 signaling, but the balance toward IgG4 is controlled by the regulatory cytokine IL-10.³³ ScRNA-seq analysis of nasal polyp cells from subjects with AERD revealed expression of *IL10* by macrophages and inflammatory DC3, with a minor contribution from the T cell compartment (**Figure S4**). Our finding that AERD polyps express more than three-fold higher levels of *IL10* mRNA (but not other B cell active cytokines) than CRSwNP tissue (**Table 2**) is consistent with regulatory T cells or myeloid cells driving IgG4 production in response to chronic antigen exposure. IgG4 may have an immunoregulatory role in patients with allergic sensitization³⁴ and is involved in the immune response to invasive parasites.³⁵ However, it is also elevated in pathologic conditions including eosinophilic esophagitis³⁶ and IgG4-related diseases, a group of fibro-inflammatory disorders involving multiple organ systems.³⁷ Given that IgG4 can potentially block antigen binding to IgE, it is also possible that it could modify skin test reactivity in patients with AERD, who are frequently non-atopic, as it may in subjects with eosinophilic esophagitis who respond clinically to food protein withdrawal even without evidence for IgE sensitization.

We then sought to identify cell type-intrinsic factors that might favor the production of IgE and IgG4 over other isotypes in AERD polyps. Massively parallel scRNA-Seq can reveal cell-type and disease-specific differences in mRNA expression profiles by revealing the most strongly differentially expressed transcripts. Accordingly, we identified distinct clusters of antibody-secreting cells in AERD notable for their strong expressions of *IGHG4* and *IGHE* and also distinguished by *IL5RA* expression (**Figure 3B and 3C**). We verified that AERD polyps contained substantially greater numbers and percentages of plasma cells bearing surface IL-5R α than did CRSwNP control polyps (**Figure 4C**), and we found that nasal polyp antibody-secreting cells in subjects with AERD express both IL-5R α and IgG4 (**Figure 4D**). Though best known for its survival-sustaining effects on eosinophils, IL-5 was originally described as a factor required for the activation, proliferation, and differentiation of mouse B cells into antibody-secreting plasma cells,³⁸⁻⁴⁰ and acts as a strong survival factor for mouse plasma cells.⁴¹ Further, IL-5 has been shown to act synergistically with IL-4 to increase lymphocyte production of IgE from human lymphocytes *in vitro*⁴² and IL-5 production is known to be associated with IgE levels in humans *in vivo*.⁴³ We suspect that IL-5 signals selectively to plasma cells that generate both IgE and IgG4, potentially sustaining their survival and promoting antibody production. What selectively regulates the expression of IL-5R α on IgG4 and IgE-secreting cells will be of great interest to determine.

Humanized monoclonal antibodies against IL-5 and IL-5R α show efficacy in the treatment of eosinophilic asthma and nasal polyposis.^{44,45} A Phase 2 trial of IL-5 inhibition with mepolizumab in patients with nasal polyposis showed a therapeutic effect with a reduction in both polyp size and patient symptoms,⁴⁶ and we recently demonstrated that mepolizumab improved upper respiratory symptoms and asthma control in subjects with AERD.⁴⁷ However, another recent study of dexamipexole, an experimental drug that depletes nearly all eosinophils from within the nasal polyp tissue, failed to show any symptomatic improvement or any reduction in nasal polyp size.⁴⁸ Taken together with our current findings, we suspect that IL-5-targeting monoclonal antibodies may alter the survival and function of IL-5R α^+ antibody-secreting cells, which may contribute to the mechanism of their therapeutic benefit.

Table 1. Patient characteristics.

	AERD	CRSwNP	CRSsNP	Healthy Controls
Number	n = 37	n = 28	N = 13	N = 5
Sex (male:female)	17:20	17:11	4:9	0:5
Median age (y) [range]	47 [21-71]	52 [20-74]	31 [23-67]	41 [31-67]
Asthma (%)	100%	25%	38%	0
Lifetime number of polypectomies (mean ±SD)	2.5 (\pm 1.3)	1.3 (\pm 0.4)*	N/A	N/A

* This is p < 0.0001 for CRSwNP lifetime number of polyp surgeries compared to the AERD lifetime number of polyp surgeries

Figure 1. Nasal tissue antibody levels are elevated in AERD and correlate with nasal polyp recurrence. Total tissue levels of (A) IgA, (B) IgG, and (C) IgE were measured by ELISA from concha bullosa samples of patients without sinus inflammation (healthy controls), sinus mucosa of patients with CRSsNP, and nasal polyp tissue from patients with aspirin-tolerant CRSwNP and AERD. The nasal polyp immunoglobulin levels from patients with aspirin-tolerant CRSwNP and AERD correlate with lifetime number of polyp surgeries (D-F). Data in A-C are mean \pm SEM, correlation in D-F was calculated by Spearman.

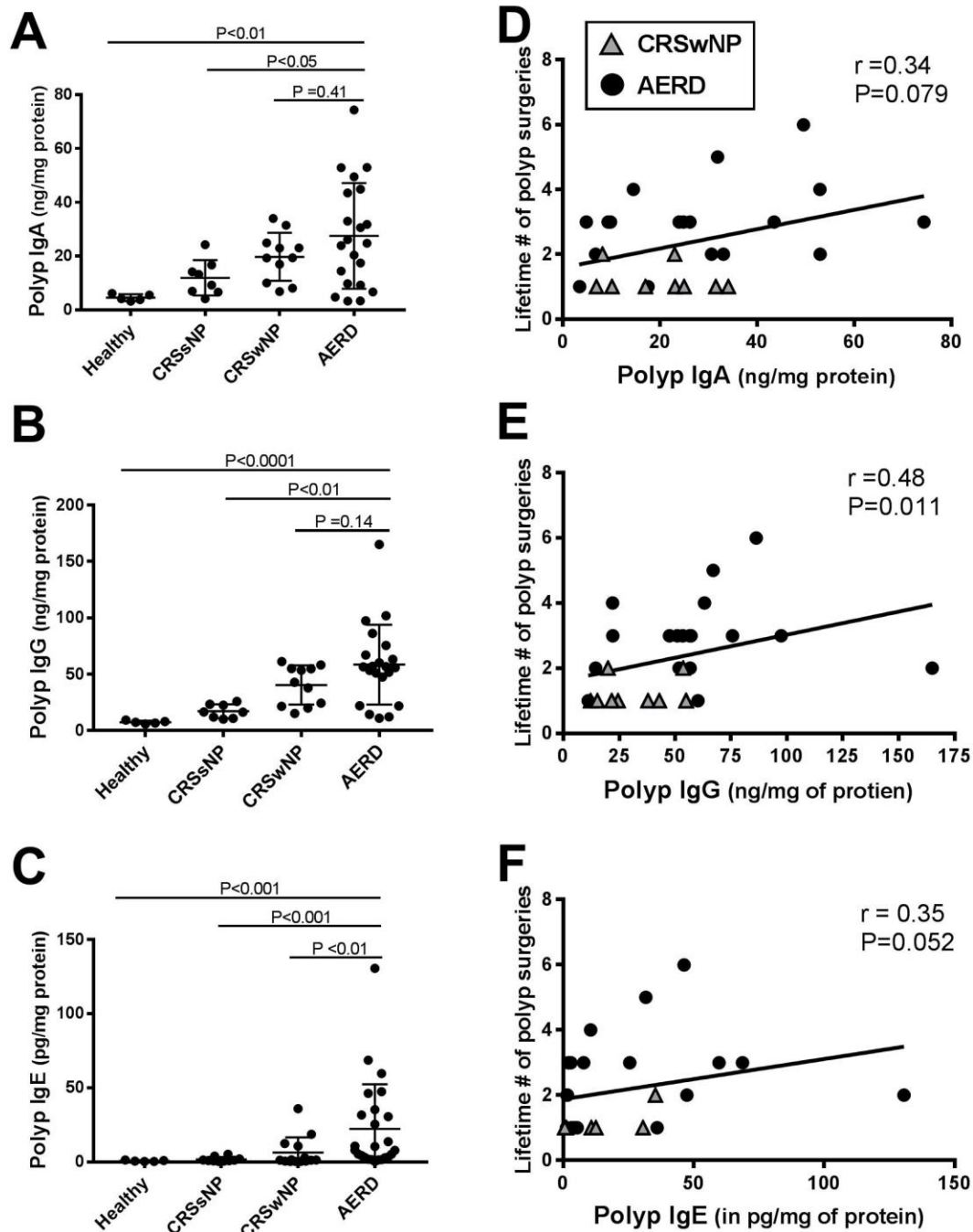


Figure 2. IgG4 isotype and IgG4⁺ antibody-secreting cells are specifically elevated in nasal polyps from patients with AERD. (A) IgG4 levels measured in tissue lysates from healthy patients without sinus inflammation, sinus mucosa of patients with CRSsNP, and nasal polyp tissue from patients with aspirin-tolerant CRSwNP and AERD. (B) Nasal polyp IgG4 levels from patients with aspirin-tolerant CRSwNP and AERD correlate with lifetime number of polyp surgeries. (C) Number of IgG4⁺ lymphocytes per HPF from nasal polyp tissue of patients with aspirin-tolerant CRSwNP and AERD, n=5 for each group. Data in A and C are mean \pm SEM. (D, E) Representative samples (CRSwNP, D and AERD, E) of nasal polyp tissue stained with anti-IgG4. Black arrows identify IgG4⁺ cells.

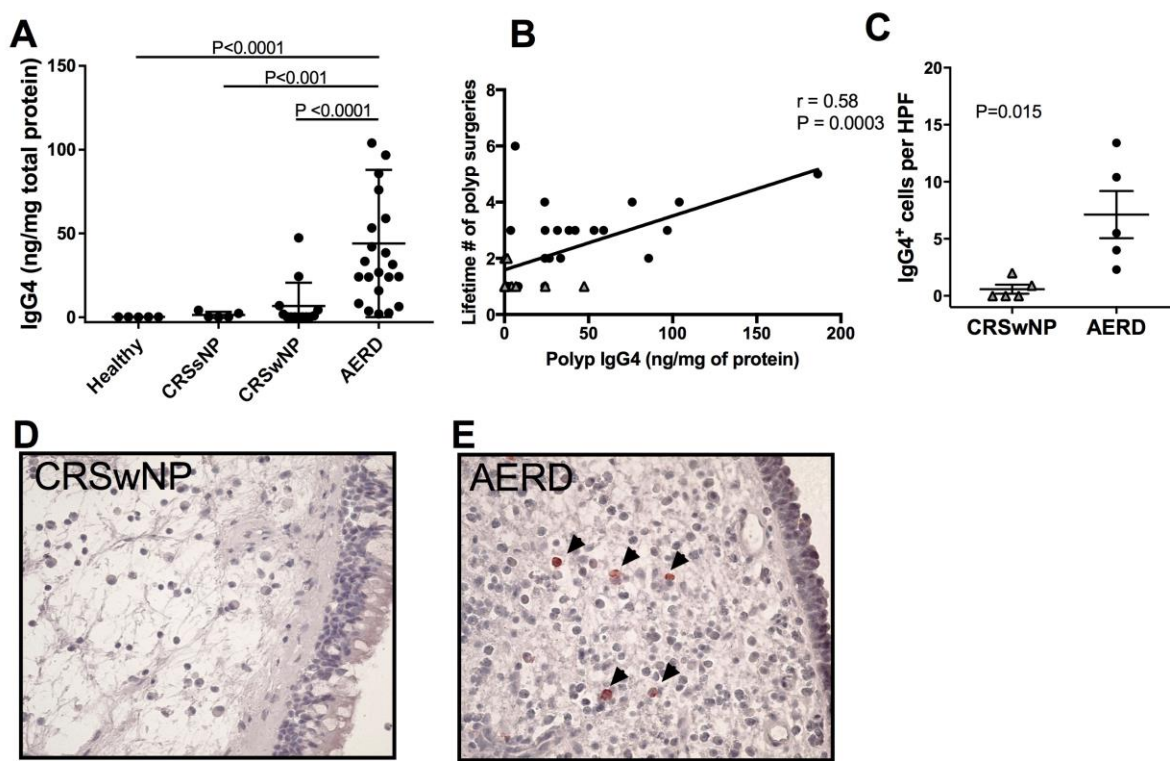


Table 2. Whole polyp qPCR for Type 2 cytokine and B cell-related genes. Expression of cytokine transcripts in whole nasal polyp tissue specimens is shown for a panel of B cell active cytokines, normalized to glyceraldehyde-3-phosphate dehydrogenase; unpaired, 2-tailed *t*-test.

	AERD	Number	CRSwNP	Number	P-value
<i>IL4</i>	0.0016 ± 0.00075	13	0.00037± 8.526e-005	9	0.20
<i>IL5</i>	0.088 ± 0.047	8	0.0065 ± 0.0026	8	0.10
<i>IL6</i>	0.079 ± 0.032	8	0.0069 ± 0.0028	8	0.07
<i>IL7</i>	0.0090 ± 0.015	8	0.0060 ± 0.0064	8	0.65
<i>IL10</i>	0.0017 ± 0.00045	13	0.00047 ± 0.00012	9	0.037
<i>IL13</i>	0.0010 ± 0.00052	13	0.00094 ± 0.00060	9	0.91
<i>IL23</i>	0.065 ± 0.087	8	0.018 ± 0.025	8	0.23
<i>TGFB1</i>	0.025 ± 0.017	8	0.025 ± 0.012	8	0.87
<i>IFNA1</i>	0.0013 ± 0.00078	8	0.0015 ± 0.0024	8	0.84
<i>CXCL12</i>	0.36 ± 0.0070	9	0.031 ± 0.0083	7	0.65
<i>CXCL13</i>	0.0015 ± 0.00046	9	0.0046	7	0.27
<i>PRDM1</i>	0.012 ± 0.0028	9	0.020 ± 0.0084	7	0.31
<i>TNFSF13B</i>	0.0017 ± 0.0017	9	0.0028 ± 0.00082	7	0.17

Figure 3. ScRNA-Seq of antibody secreting-cell populations from sinus tissue of subjects with CRSsNP (n=5), CRSwNP (n=3) and AERD (n=3). A. UMAP plot of 2,520 antibody-secreting cells from sinonal nasal tissue of CRSsNP, CRSwNP and AERD patients, indicating 9 clusters identified through a shared nearest neighbor analysis. B. UMAP plot of sinonal nasal antibody-secreting cells, colored by disease of origin. Statistical enrichment for AERD disease-of-origin was observed for cluster 2 ($p<1\times10^{-15}$), cluster 3 ($p<1\times10^{-15}$), cluster 4 ($p<2\times10^{-12}$), cluster 6 ($p<1\times10^{-15}$), and cluster 7 ($p<1\times10^{-15}$). C. Violin plots of select genes significantly enriched in AERD relative to CRSsNP and CRSwNP within sinonal nasal antibody-secreting cell populations, including *IGHG4* ($p<1\times10^{-201}$), *IGHE* ($p<2\times10^{-34}$), and *IL5RA* ($p<2\times10^{-21}$). Cohen's d effect size for AERD relative to CRSwNP is 1.57, 0.50, and 0.37, respectively for the 3 transcripts.

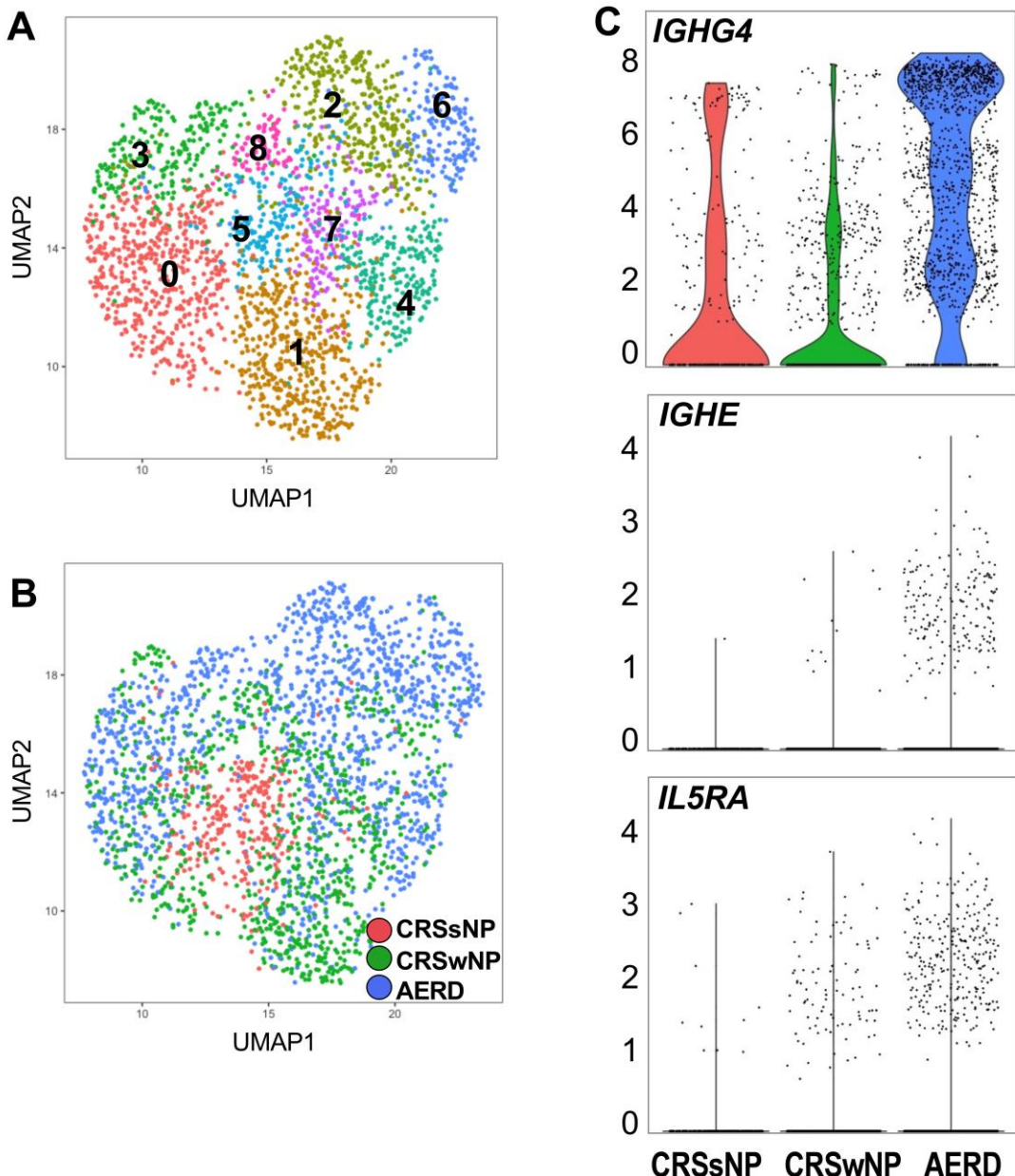
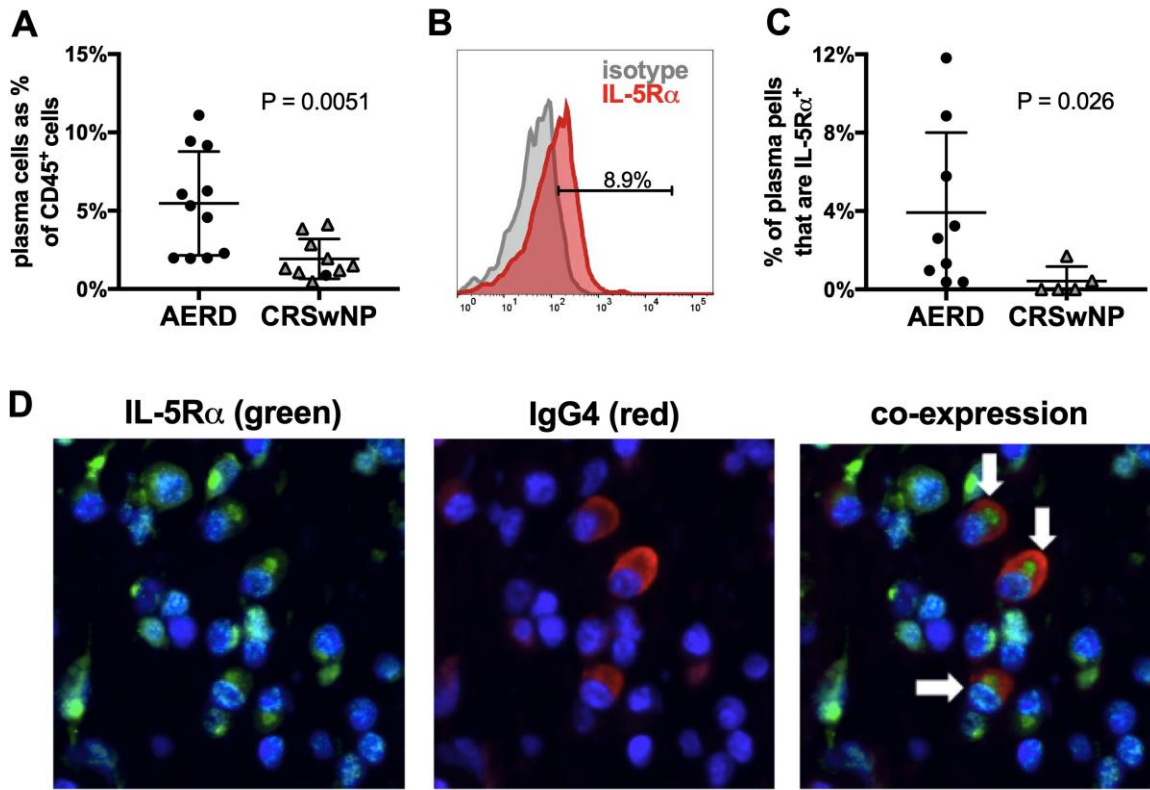
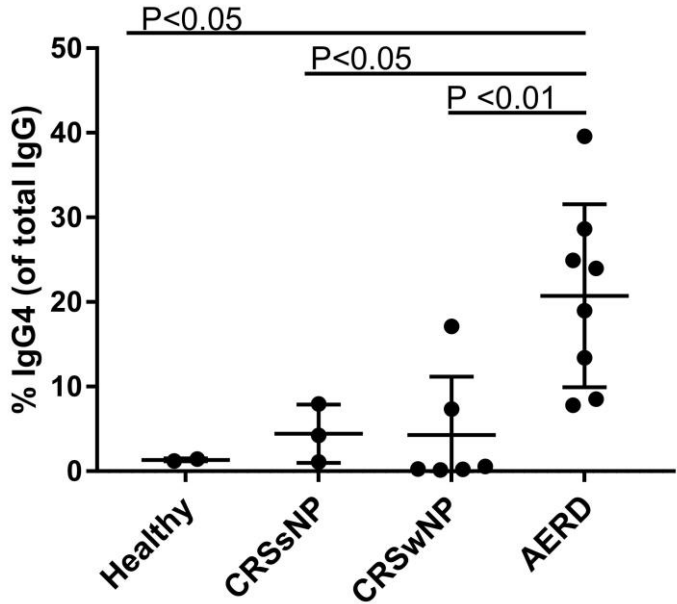


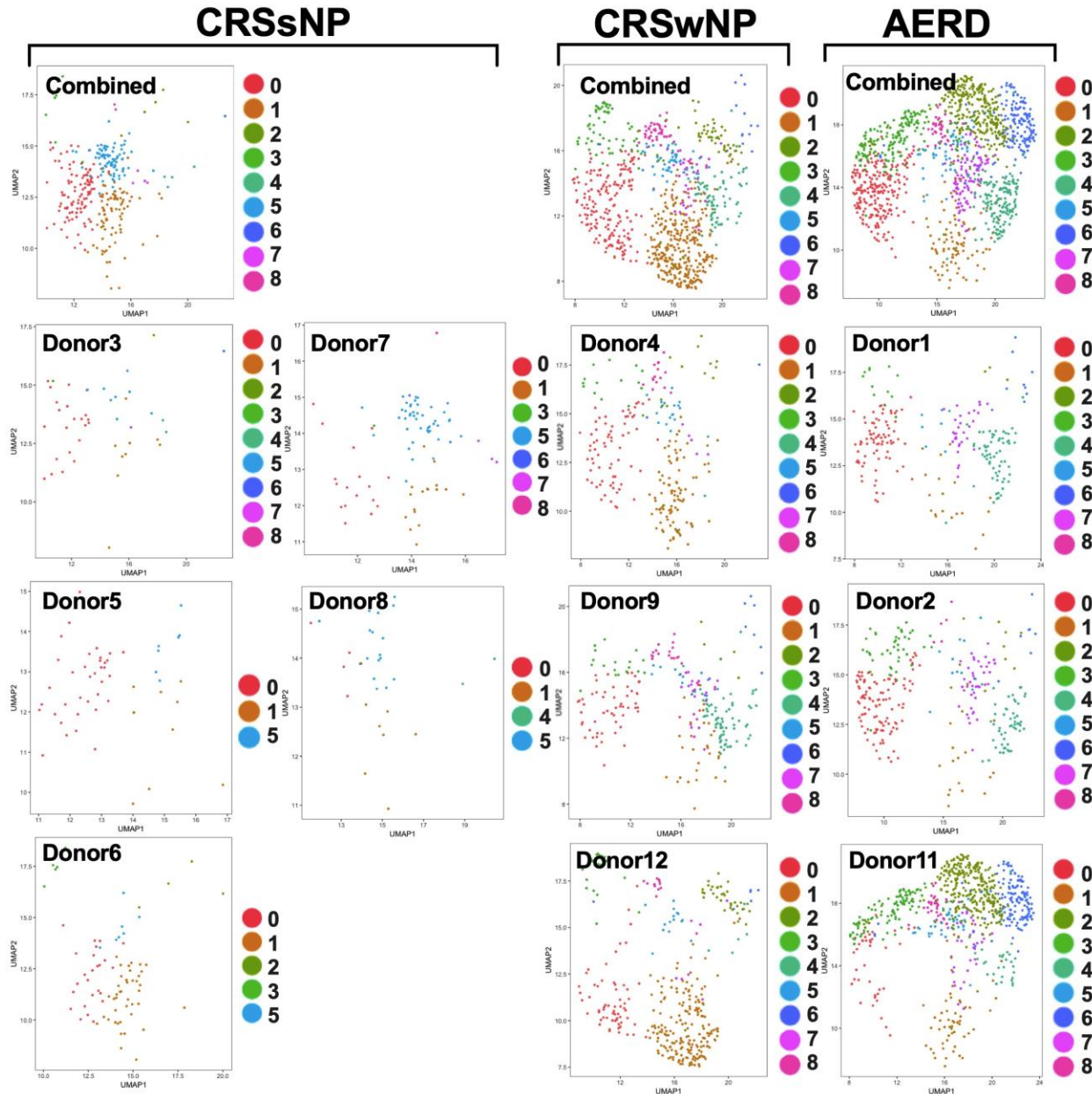
Figure 4. Flow cytometric characterization of plasma cells and immunofluorescence of polyp tissue. (A) Nasal polyp plasma cell frequency as a percentage of CD45⁺ cells, (B) representative histogram of IL-5R α surface expression (with isotype positivity subtracted) on plasma cells from an AERD patient, (C) plasma cell surface expression of IL-5R α , and (D) immunofluorescence staining of nasal polyp tissue for plasma cells (white arrows) co-expressing IL-5R α (green) and IgG4 (red).



Supplementary Figure 1. IgG4 levels measured in tissue lysates as a percent of total IgG tissue lysate levels from healthy patients without sinus inflammation, sinus mucosa of patients with CRSsNP, and nasal polyp tissue from patients with aspirin-tolerant CRSwNP and AERD. Data are mean \pm SEM.

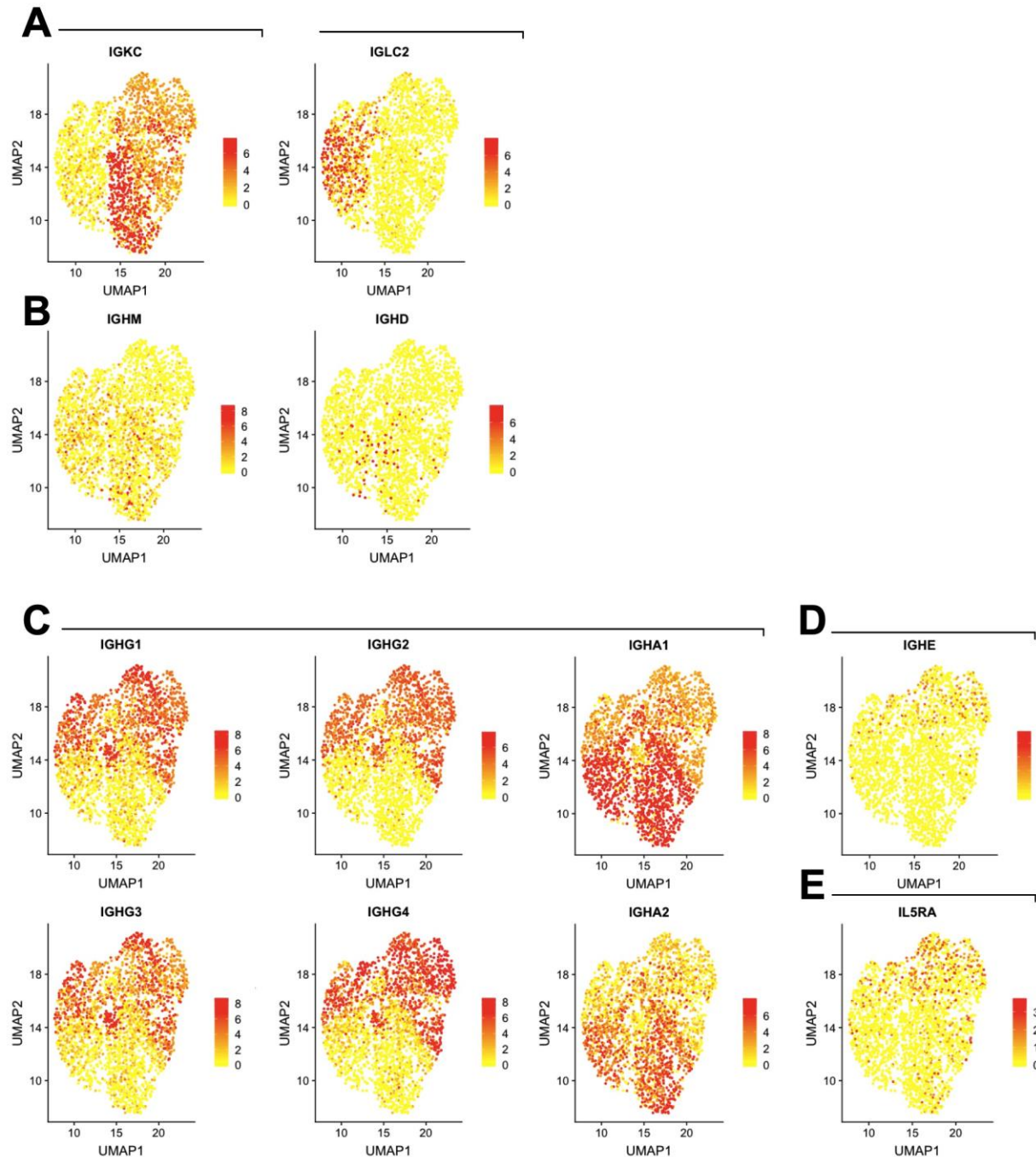


Supplementary Figure 2. UMAP plots of 2,520 antibody-secreting cells colored by cluster as identified in **Fig. 3** and separated by disease (CRSsNP: 297 cells, CRSwNP: 835 cells, AERD: 1388 cells) and individual donor (Donor 1: 226 cells, Donor 2: 398 cells, Donor 3: 46 cells, Donor 4: 232 cells, Donor 5: 52 cells, Donor 6: 83 cells, Donor 7: 84 cells, Donor 8: 32 cells, Donor 9: 242 cells, Donor 11: 764 cells, Donor 12: 361 cells).



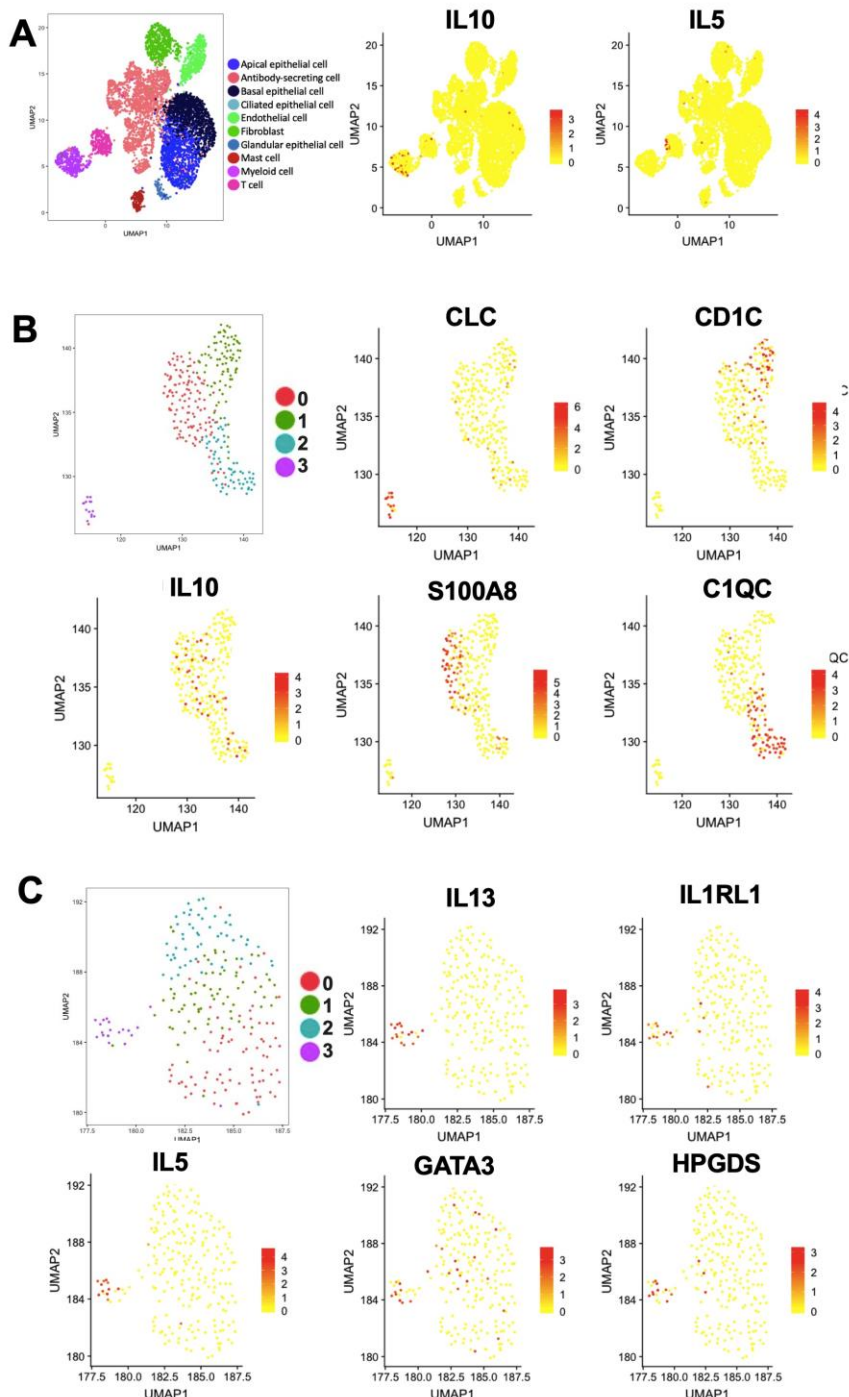
Supplementary Figure 3.

UMAP of 2,520 antibody-secreting cells, colored by expression of (A) Light chain constant regions (*IGKC*, *IGLC2*), (B) Non-class-switched heavy chain constant regions (*IGHM*, *IGHD*), (C) class-switched IgG and IgA isotype heavy chain regions (*IGHG1*, *IGHG2*, *IGHG3*, *IGHG4*, *IGHA1*, *IGHA2*), (D) the immunoglobulin E heavy chain (*IGHE*), and (E) the IL-5 receptor alpha chain (*IL5RA*). Scale indicates log-normalized expression.



Supplementary Figure 4.

UMAP plot of 4,276 nasal polyp cells from subjects with AERD (n=3 samples), colored by cell type (left) and IL5 and IL10 expression (right) **(B)** UMAP plot of 282 myeloid lineage derived from (A), clustered with accompanying plots to show *IL10* expression across sub-populations including *S100A8*-expressing inflammatory DC3 (Cluster 0) and *C1QC*-expressing macrophages (cluster 2), but not including *CLC*-expressing eosinophils (cluster 3) or *CD1C*-expressing DC2 (cluster1). **(C)** UMAP plot of 224 T lymphocytes derived from (A), clustered with accompanying plots to show *IL5* expression within cluster 3, which additionally expressed *IL13*, *IL1RL1*, *GATA3* and *HPGDS*, suggesting a Th2A phenotype. Scale indicates log-normalized expression.



Supplemental Table E1. Antibody-secreting cell cluster defining genes.

	p_val	avg_logFC	pct.1	pct.2	p_val_adj	cluster	gene
IGLC7	2.77E-216	2.21906487	0.981	0.299	8.59E-212	0	IGLC7
IGLL1	4.68E-198	2.05069445	0.935	0.252	1.45E-193	0	IGLL1
IGLC3	1.82E-170	1.70404197	0.91	0.229	5.64E-166	0	IGLC3
GUSBP11	1.38E-158	1.95998104	0.731	0.129	4.29E-154	0	GUSBP11
IGLC2	7.11E-120	2.21368634	0.662	0.181	2.21E-115	0	IGLC2
IGLV2-14	1.37E-85	3.59931063	0.363	0.047	4.24E-81	0	IGLV2-14
IGLV2-8	1.14E-80	2.80209198	0.347	0.033	3.53E-76	0	IGLV2-8
IGLV2-18	1.79E-79	2.03962886	0.311	0.021	5.56E-75	0	IGLV2-18
IGLV2-23	7.98E-79	2.67662976	0.351	0.04	2.48E-74	0	IGLV2-23
D86994.2	8.40E-68	2.78586089	0.228	0.01	2.61E-63	0	D86994.2
IGLJ2	8.49E-57	2.36387458	0.303	0.043	2.63E-52	0	IGLJ2
IGLV2-33	5.48E-56	1.79192864	0.184	0.006	1.70E-51	0	IGLV2-33
IGLV2-11	2.10E-46	1.63722599	0.286	0.05	6.52E-42	0	IGLV2-11
IGHA1	2.66E-43	0.54060025	0.969	0.943	8.24E-39	0	IGHA1
IGLJ3	2.81E-40	2.02593594	0.305	0.067	8.72E-36	0	IGLJ3
KREMEN1	6.35E-39	0.85813394	0.221	0.035	1.97E-34	0	KREMEN1
IGLV3-25	5.15E-24	2.04284728	0.177	0.04	1.60E-19	0	IGLV3-25
D87024.1	3.81E-22	0.86582483	0.142	0.028	1.18E-17	0	D87024.1
IGLV1-40	4.77E-22	1.40596643	0.192	0.05	1.48E-17	0	IGLV1-40
IGLV1-36	6.04E-22	1.4826307	0.136	0.023	1.87E-17	0	IGLV1-36
IGLV3-10	7.85E-19	1.75237163	0.109	0.017	2.44E-14	0	IGLV3-10
IGLV3-21	3.16E-16	1.9812743	0.19	0.074	9.80E-12	0	IGLV3-21
IGLL5	6.85E-16	1.98891376	0.403	0.325	2.12E-11	0	IGLL5
IGLV6-57	8.79E-15	0.89635746	0.33	0.171	2.73E-10	0	IGLV6-57
IGLV1-47	4.62E-14	1.60542993	0.152	0.049	1.43E-09	0	IGLV1-47
IGLV3-9	5.27E-13	2.24406002	0.119	0.033	1.64E-08	0	IGLV3-9
AL928768.3	2.02E-12	0.29891436	0.269	0.128	6.26E-08	0	AL928768.3
IGLV1-50	6.58E-12	0.4801471	0.107	0.029	2.04E-07	0	IGLV1-50
IGHV3-74	1.42E-11	1.11946964	0.167	0.075	4.42E-07	0	IGHV3-74
IGLV3-19	3.39E-11	1.71538449	0.104	0.03	1.05E-06	0	IGLV3-19
RNA18S5	2.77E-10	0.35714429	0.436	0.295	8.58E-06	0	RNA18S5
IGHD	4.04E-07	1.17374501	0.142	0.07	0.01253251	0	IGHD
IGLV1-44	4.63E-07	0.55461695	0.113	0.046	0.01435659	0	IGLV1-44
IGHA11	1.36E-84	1.00096099	0.96	0.946	4.23E-80	1	IGHA1
IGHA2	1.36E-71	1.10546868	0.901	0.708	4.21E-67	1	IGHA2
IGKV1-271	4.73E-25	1.79413866	0.213	0.073	1.47E-20	1	IGKV1-27
IGJ	2.07E-21	0.4752816	0.98	0.981	6.41E-17	1	IGJ
ENAM	2.38E-13	0.35676009	0.83	0.726	7.39E-09	1	ENAM

RGS1	3.56E-12	0.49102791	0.747	0.673	1.11E-07	1	RGS1
HERPUD1	9.57E-11	0.34419163	0.846	0.808	2.97E-06	1	HERPUD1
TTC26	3.82E-08	0.42749194	0.168	0.09	0.00118554	1	TTC26
RGS2	7.67E-08	0.47285389	0.344	0.251	0.00238057	1	RGS2
IGKV1-51	1.27E-06	0.50331469	0.251	0.17	0.0393702	1	IGKV1-5
IGKV3-202	3.33E-79	1.06063111	0.761	0.22	1.03E-74	2	IGKV3-20
IGHG12	2.83E-78	1.3666138	0.977	0.633	8.77E-74	2	IGHG1
IGHG22	2.18E-69	0.86513112	0.974	0.487	6.77E-65	2	IGHG2
IGHV4-392	1.68E-67	1.84832305	0.513	0.118	5.23E-63	2	IGHV4-39
IGHG42	1.53E-62	0.75634877	0.977	0.592	4.76E-58	2	IGHG4
FBRSL1	9.11E-55	1.41701537	0.296	0.031	2.83E-50	2	FBRSL1
IGHG32	7.47E-53	1.00030318	0.94	0.647	2.32E-48	2	IGHG3
BNIP32	3.80E-52	1.58448519	0.333	0.055	1.18E-47	2	BNIP3
FHDC1	6.06E-38	0.90180961	0.211	0.02	1.88E-33	2	FHDC1
AC096579.71	1.78E-33	0.69157037	0.795	0.533	5.51E-29	2	AC096579.7
IGKV3D-202	8.31E-32	0.67440194	0.453	0.147	2.58E-27	2	IGKV3D-20
CCND22	6.85E-22	0.67273435	0.638	0.402	2.12E-17	2	CCND2
IGKV5-2	9.08E-21	0.50249632	0.108	0.01	2.82E-16	2	IGKV5-2
IGHV4OR15-8	4.42E-18	0.55372926	0.217	0.054	1.37E-13	2	IGHV4OR15-8
DPEP1	6.83E-17	0.52444555	0.185	0.048	2.12E-12	2	DPEP1
IL5RA2	8.82E-16	0.63182185	0.316	0.147	2.74E-11	2	IL5RA
IGHV4-341	4.27E-11	1.65186055	0.174	0.079	1.33E-06	2	IGHV4-34
IGHE1	4.00E-10	0.47091036	0.174	0.067	1.24E-05	2	IGHE
IGKV3-72	1.17E-09	0.37363639	0.254	0.117	3.62E-05	2	IGKV3-7
IGHV1-241	1.18E-08	0.60271341	0.356	0.21	0.00036529	2	IGHV1-24
IGKV3D-7	1.40E-08	0.36709825	0.148	0.056	0.00043403	2	IGKV3D-7
QTRTD1	2.30E-08	0.4028371	0.117	0.043	0.00071244	2	QTRTD1
FAM92B	4.14E-08	0.41354248	0.128	0.055	0.00128404	2	FAM92B
PRDX41	7.74E-08	0.2972605	0.806	0.754	0.00240111	2	PRDX4
CD91	4.55E-07	0.36146568	0.393	0.283	0.0141117	2	CD9
GTF3A1	5.62E-07	0.35529178	0.45	0.348	0.01744403	2	GTF3A
GAS61	1.07E-06	0.41900607	0.251	0.164	0.03313202	2	GAS6
IGLC33	3.31E-81	1.5298387	0.942	0.317	1.03E-76	3	IGLC3
IGLL13	2.89E-76	1.12940085	0.969	0.341	8.97E-72	3	IGLL1
IGLC73	1.31E-69	0.98009448	0.973	0.392	4.06E-65	3	IGLC7
GUSBP113	4.17E-44	1.02024974	0.711	0.212	1.30E-39	3	GUSBP11
IGHG23	1.32E-42	0.72175196	0.973	0.515	4.10E-38	3	IGHG2
IGHG13	1.73E-41	0.76762382	0.991	0.652	5.37E-37	3	IGHG1
IGHG33	8.96E-35	0.7736927	0.96	0.662	2.78E-30	3	IGHG3
IGHG43	1.43E-32	0.66506827	0.982	0.614	4.44E-28	3	IGHG4

IGHV3-212	3.86E-31	2.16071991	0.476	0.19	1.20E-26	3	IGHV3-21
IGLC23	2.58E-29	1.02325202	0.644	0.247	8.01E-25	3	IGLC2
IGLV6-573	3.96E-28	2.35865074	0.436	0.182	1.23E-23	3	IGLV6-57
IGLV1-441	9.78E-27	2.59091733	0.253	0.041	3.04E-22	3	IGLV1-44
IGLV4-60	2.55E-24	1.39276687	0.16	0.011	7.91E-20	3	IGLV4-60
IGLJ33	2.18E-23	1.00609974	0.351	0.095	6.77E-19	3	IGLJ3
IGLV4-69	7.63E-21	2.35933361	0.187	0.028	2.37E-16	3	IGLV4-69
IGLV1-501	7.44E-18	1.13068528	0.196	0.031	2.31E-13	3	IGLV1-50
IGLV1-471	3.34E-17	1.48244341	0.227	0.055	1.04E-12	3	IGLV1-47
IGHV3-38	1.90E-15	0.79601754	0.227	0.059	5.90E-11	3	IGHV3-38
KREMEN11	4.73E-14	0.60034168	0.236	0.059	1.47E-09	3	KREMEN1
IGLV1-401	1.23E-12	1.63960021	0.213	0.067	3.82E-08	3	IGLV1-40
IGLV3-213	3.73E-12	0.67544671	0.267	0.082	1.16E-07	3	IGLV3-21
IGLV3-27	9.99E-10	0.65931111	0.111	0.023	3.10E-05	3	IGLV3-27
IGLJ23	1.83E-09	0.7480763	0.227	0.086	5.67E-05	3	IGLJ2
IGLV1-361	2.71E-09	0.31272529	0.147	0.037	8.41E-05	3	IGLV1-36
IGHV3-642	3.22E-08	1.12166682	0.231	0.1	0.00099873	3	IGHV3-64
IGHV3OR16-8	7.37E-07	0.82052111	0.12	0.039	0.02286137	3	IGHV3OR16-8
IGKV1OR2-1083	5.60E-137	2.78574189	0.884	0.114	1.74E-132	4	IGKV1OR2-108
IGKV1-63	9.55E-114	2.79311622	0.72	0.057	2.96E-109	4	IGKV1-6
IGKV1-39	1.37E-99	2.69637035	0.502	0.018	4.24E-95	4	IGKV1-39
IGKV1D-8	5.16E-96	3.3994364	0.547	0.032	1.60E-91	4	IGKV1D-8
IGKV1-163	1.56E-85	2.54620336	0.569	0.048	4.85E-81	4	IGKV1-16
IGKV1-54	2.13E-78	2.35940462	0.756	0.129	6.62E-74	4	IGKV1-5
IGKV1D-17	1.08E-68	2.19419328	0.409	0.023	3.36E-64	4	IGKV1D-17
IGKV1D-39	6.82E-66	2.37747591	0.351	0.013	2.12E-61	4	IGKV1D-39
IGKV1-91	1.66E-57	3.21568558	0.444	0.048	5.15E-53	4	IGKV1-9
IGKV1D-12	5.73E-54	2.16331121	0.293	0.01	1.78E-49	4	IGKV1D-12
IGKV1-81	4.07E-53	1.61954065	0.444	0.049	1.26E-48	4	IGKV1-8
IGKV1D-16	9.49E-53	1.18448871	0.36	0.023	2.94E-48	4	IGKV1D-16
IGKV1D-422	2.05E-51	1.84228432	0.467	0.073	6.36E-47	4	IGKV1D-42
CH17-132F21.1	1.16E-49	1.32872588	0.316	0.017	3.60E-45	4	CH17-132F21.1
IGKV1D-43	1.58E-48	2.37050596	0.369	0.028	4.90E-44	4	IGKV1D-43
IGKV1-17	9.46E-47	2.66312918	0.391	0.035	2.93E-42	4	IGKV1-17
IGKV1D-13	7.36E-44	2.16198066	0.284	0.019	2.28E-39	4	IGKV1D-13
IGKV1-12	7.04E-41	2.32770668	0.289	0.02	2.18E-36	4	IGKV1-12
IGKV1D-33	1.26E-21	1.18661271	0.156	0.012	3.91E-17	4	IGKV1D-33
IGKV1-274	7.20E-19	0.77590341	0.356	0.076	2.23E-14	4	IGKV1-27
IGKV1-33	3.95E-18	0.83258944	0.142	0.011	1.23E-13	4	IGKV1-33

AC096579.73	2.67E-17	1.2116291	0.8	0.548	8.30E-13	4	AC096579.7
IGHV3-233	9.12E-17	1.56974492	0.453	0.234	2.83E-12	4	IGHV3-23
MTRNR2L21	3.27E-16	0.59434187	0.809	0.552	1.02E-11	4	MTRNR2L2
IGKV1-37	5.69E-16	0.38358843	0.111	0.006	1.77E-11	4	IGKV1-37
IGHV3-53	2.32E-14	1.8891805	0.213	0.062	7.19E-10	4	IGHV3-53
RPS272	3.20E-13	0.46433491	0.778	0.551	9.94E-09	4	RPS27
MTRNR2L121	1.76E-12	0.50957473	0.778	0.567	5.46E-08	4	MTRNR2L12
IGHV3-483	3.14E-12	0.74664779	0.347	0.148	9.74E-08	4	IGHV3-48
RNA28S52	9.91E-12	0.34249552	0.969	0.938	3.08E-07	4	RNA28S5
IGHV3OR16-131	3.03E-11	0.65434353	0.2	0.057	9.40E-07	4	IGHV3OR16-13
RPL172	1.15E-10	0.52502017	0.489	0.279	3.56E-06	4	RPL17
IGHV4-61	7.64E-10	0.9396053	0.138	0.029	2.37E-05	4	IGHV4-61
IGHV3OR16-10	1.53E-09	0.52490056	0.178	0.058	4.74E-05	4	IGHV3OR16-10
RPL101	2.30E-09	0.33322602	0.849	0.685	7.13E-05	4	RPL10
RPL41	2.46E-09	0.26457064	0.942	0.869	7.65E-05	4	RPL41
RPL36	3.34E-09	0.33654798	0.813	0.63	0.00010366	4	RPL36
IGHV3-213	4.33E-09	0.95173704	0.364	0.201	0.00013444	4	IGHV3-21
MTRNR2L3	5.13E-09	0.50106049	0.538	0.342	0.00015912	4	MTRNR2L3
MALAT11	7.01E-09	0.48787715	0.982	0.944	0.00021749	4	MALAT1
IGHV4-4	4.10E-08	1.43572464	0.169	0.071	0.00127331	4	IGHV4-4
IGHV3-643	5.39E-08	0.47020069	0.231	0.1	0.00167197	4	IGHV3-64
RPL18A	5.65E-08	0.34892893	0.689	0.512	0.00175191	4	RPL18A
MTRNR2L1	6.54E-08	0.33063003	0.867	0.74	0.00203036	4	MTRNR2L1
MTRNR2L81	7.68E-08	0.34989524	0.831	0.67	0.00238431	4	MTRNR2L8
IGHV3OR16-123	4.62E-07	0.64279532	0.227	0.103	0.01433353	4	IGHV3OR16-12
PLAUR	7.29E-07	0.33521796	0.173	0.071	0.02262866	4	PLAUR
IGHV3OR15-7	1.03E-06	0.68132776	0.16	0.064	0.03209963	4	IGHV3OR15-7
SLPI2	1.51E-41	1.12791709	0.937	0.544	4.69E-37	5	SLPI
STATH4	2.31E-28	1.93353486	0.487	0.161	7.15E-24	5	STATH
LYZ3	1.23E-24	1.49962766	0.429	0.128	3.81E-20	5	LYZ
PERP1	5.56E-20	0.83678505	0.429	0.135	1.72E-15	5	PERP
BPIFB11	5.34E-19	1.02000705	0.582	0.291	1.66E-14	5	BPIFB1
EGR1	1.52E-17	0.59491839	0.693	0.359	4.70E-13	5	EGR1
AGR21	2.35E-17	0.89017331	0.418	0.152	7.29E-13	5	AGR2
IGKC4	1.09E-16	1.15203741	0.794	0.671	3.37E-12	5	IGKC
BPIFA11	3.13E-16	1.08793137	0.646	0.388	9.72E-12	5	BPIFA1
EPAS1	3.67E-16	0.72635267	0.265	0.057	1.14E-11	5	EPAS1
F31	5.37E-16	0.7464354	0.344	0.114	1.67E-11	5	F3

SERPINB32	7.94E-16	1.20921605	0.524	0.292	2.46E-11	5	SERPINB3
ATP1B1	8.95E-16	0.70736782	0.254	0.058	2.78E-11	5	ATP1B1
ZG16B	3.66E-15	0.65259716	0.259	0.06	1.14E-10	5	ZG16B
GLUL	5.83E-15	0.67951581	0.291	0.081	1.81E-10	5	GLUL
S100A6	1.41E-14	0.77507949	0.735	0.514	4.38E-10	5	S100A6
S100A22	1.57E-14	1.19535035	0.45	0.232	4.86E-10	5	S100A2
CP	3.13E-14	0.65539738	0.175	0.029	9.70E-10	5	CP
ADIRF	3.35E-14	0.57793468	0.27	0.066	1.04E-09	5	ADIRF
LTF	4.77E-14	0.75473702	0.222	0.045	1.48E-09	5	LTF
PIGR1	8.97E-14	0.8597608	0.344	0.113	2.78E-09	5	PIGR
ZFP36L1	2.55E-13	0.54761239	0.381	0.136	7.92E-09	5	ZFP36L1
KRT5	4.64E-13	0.76559249	0.222	0.057	1.44E-08	5	KRT5
NCOA7	6.95E-13	0.73637546	0.381	0.163	2.16E-08	5	NCOA7
IGKJ32	7.37E-13	1.31459458	0.243	0.076	2.29E-08	5	IGKJ3
MSMB	8.51E-13	0.58092354	0.259	0.062	2.64E-08	5	MSMB
CXADR	1.46E-12	0.44455019	0.116	0.011	4.54E-08	5	CXADR
SAT11	2.33E-12	0.53763693	0.688	0.408	7.24E-08	5	SAT1
ANXA2	2.37E-12	0.7199335	0.471	0.228	7.36E-08	5	ANXA2
IGHG35	3.21E-12	0.917804	0.794	0.681	9.96E-08	5	IGHG3
KRT18	3.40E-12	0.62880906	0.233	0.061	1.05E-07	5	KRT18
ITM2B	6.35E-12	0.45382796	0.646	0.368	1.97E-07	5	ITM2B
HES1	7.62E-12	0.60393742	0.196	0.046	2.36E-07	5	HES1
ADH7	1.23E-11	0.4783981	0.106	0.013	3.82E-07	5	ADH7
JUN1	2.14E-11	0.41839397	0.905	0.755	6.64E-07	5	JUN
ALOX151	2.37E-11	0.99629054	0.307	0.145	7.34E-07	5	ALOX15
SPINT2	2.65E-11	0.59907378	0.354	0.142	8.21E-07	5	SPINT2
PRSS23	3.23E-11	0.64493696	0.302	0.105	1.00E-06	5	PRSS23
ETS2	3.83E-11	0.60259049	0.259	0.086	1.19E-06	5	ETS2
SERPINF1	5.70E-11	0.56791456	0.228	0.07	1.77E-06	5	SERPINF1
IER3	1.02E-10	0.51119895	0.376	0.143	3.17E-06	5	IER3
KRT191	1.35E-10	0.67730499	0.534	0.317	4.18E-06	5	KRT19
KRT17	1.35E-10	0.59608521	0.127	0.022	4.20E-06	5	KRT17
ID1	1.79E-10	0.6094834	0.333	0.136	5.54E-06	5	ID1
CALM2	1.83E-10	0.46635016	0.545	0.279	5.67E-06	5	CALM2
GADD45B	2.56E-10	0.48146848	0.55	0.286	7.93E-06	5	GADD45B
WFDC2	3.65E-10	0.6733585	0.429	0.216	1.13E-05	5	WFDC2
FXYD3	3.72E-10	0.60827446	0.429	0.211	1.15E-05	5	FXYD3
CD92	4.96E-10	0.67329818	0.481	0.284	1.54E-05	5	CD9
LIMA1	6.26E-10	0.48121482	0.185	0.044	1.94E-05	5	LIMA1
ATF3	7.47E-10	0.51892383	0.492	0.245	2.32E-05	5	ATF3

ACTG1	8.06E-10	0.44632313	0.683	0.418	2.50E-05	5	ACTG1
APP	9.42E-10	0.48411341	0.175	0.044	2.92E-05	5	APP
C6orf58	1.12E-09	0.36022302	0.122	0.019	3.47E-05	5	C6orf58
MT1E	1.13E-09	0.51400674	0.18	0.039	3.51E-05	5	MT1E
EHF	1.77E-09	0.41395569	0.148	0.029	5.49E-05	5	EHF
CXCL17	2.09E-09	0.49283288	0.217	0.06	6.49E-05	5	CXCL17
MYL12B	2.50E-09	0.55718062	0.46	0.244	7.75E-05	5	MYL12B
C19orf33	2.63E-09	0.3553919	0.143	0.026	8.15E-05	5	C19orf33
FOS	2.90E-09	0.33174649	0.921	0.813	8.99E-05	5	FOS
DSP	2.98E-09	0.36866655	0.122	0.021	9.25E-05	5	DSP
ERRFI1	3.35E-09	0.45533934	0.138	0.029	0.00010392	5	ERRFI1
MT-CYB	3.47E-09	0.54535755	0.635	0.426	0.00010783	5	MT-CYB
IGHG14	3.74E-09	0.49227352	0.815	0.672	0.00011604	5	IGHG1
POSTN2	3.97E-09	1.16519148	0.466	0.379	0.00012305	5	POSTN
CLDN1	4.27E-09	0.55142294	0.127	0.028	0.00013259	5	CLDN1
KRT151	4.42E-09	0.72315989	0.286	0.117	0.00013727	5	KRT15
CFH	4.47E-09	0.42758279	0.138	0.031	0.00013857	5	CFH
TSC22D1	6.08E-09	0.60965536	0.228	0.079	0.00018866	5	TSC22D1
IL33	7.99E-09	0.49255285	0.153	0.04	0.00024796	5	IL33
ACTB	8.86E-09	0.38934214	0.571	0.33	0.00027489	5	ACTB
KLF61	9.99E-09	0.48548095	0.741	0.551	0.00030996	5	KLF6
JUNB	1.01E-08	0.41095909	0.73	0.53	0.00031365	5	JUNB
LGALS31	1.14E-08	0.5517949	0.497	0.287	0.00035408	5	LGALS3
PTHLH	1.16E-08	0.72542255	0.212	0.077	0.0003605	5	PTHLH
AQP3	1.23E-08	0.57446929	0.36	0.167	0.00038153	5	AQP3
TACSTD22	1.26E-08	0.6820213	0.381	0.197	0.0003909	5	TACSTD2
YBX3	1.68E-08	0.37430691	0.169	0.048	0.00052132	5	YBX3
KRT8	2.01E-08	0.48317122	0.212	0.069	0.00062485	5	KRT8
UGT2A2	2.10E-08	0.40294541	0.153	0.032	0.00065313	5	UGT2A2
IFI27	2.26E-08	0.57923154	0.238	0.075	0.00070185	5	IFI27
RPS12	2.29E-08	0.2911939	0.979	0.905	0.00071166	5	RPS12
ZFP36	2.39E-08	0.31996681	0.762	0.552	0.00074245	5	ZFP36
CLU	2.53E-08	0.3999511	0.201	0.055	0.00078507	5	CLU
ALDH1A1	2.66E-08	0.51300861	0.201	0.07	0.00082525	5	ALDH1A1
CYR61	2.88E-08	0.50739146	0.153	0.04	0.00089402	5	CYR61
CDH26	2.96E-08	0.4338784	0.111	0.025	0.00091976	5	CDH26
MT-ND2	3.57E-08	0.37509174	0.614	0.378	0.00110933	5	MT-ND2
ANXA11	4.20E-08	0.55635014	0.603	0.405	0.00130299	5	ANXA1
SGK1	5.00E-08	0.50524791	0.312	0.135	0.00155222	5	SGK1
RASSF6	6.19E-08	0.4194408	0.164	0.044	0.00192159	5	RASSF6

RHOC	6.41E-08	0.38683698	0.185	0.054	0.00198808	5	RHOC
ZFAND51	6.52E-08	0.50649209	0.349	0.171	0.00202313	5	ZFAND5
MYOF	6.69E-08	0.40615825	0.122	0.024	0.00207571	5	MYOF
AZGP1	6.77E-08	0.37336857	0.111	0.018	0.00210148	5	AZGP1
IFITM1	1.09E-07	0.35762875	0.138	0.037	0.00336702	5	IFITM1
TRIM2	1.09E-07	0.31139447	0.122	0.022	0.00337951	5	TRIM2
EZR1	1.09E-07	0.380359	0.603	0.378	0.00338488	5	EZR
DNAJB1	1.09E-07	0.43371161	0.354	0.163	0.00338713	5	DNAJB1
SCGB3A1	1.25E-07	0.34711796	0.101	0.02	0.00388289	5	SCGB3A1
BCAM	1.27E-07	0.28759749	0.127	0.026	0.00393485	5	BCAM
KLF10	1.32E-07	0.50021544	0.217	0.067	0.00408258	5	KLF10
KRT7	1.44E-07	0.47128618	0.19	0.056	0.00447387	5	KRT7
TMSB101	1.69E-07	0.36170708	0.847	0.687	0.00525398	5	TMSB10
TNFSF10	1.76E-07	0.40126319	0.148	0.042	0.00546405	5	TNFSF10
KLF5	1.80E-07	0.4213404	0.169	0.044	0.00557634	5	KLF5
AQP5	1.82E-07	0.31803997	0.111	0.017	0.00566295	5	AQP5
CTSB	1.85E-07	0.50410199	0.354	0.172	0.00573774	5	CTSB
IFITM3	2.34E-07	0.563426	0.27	0.111	0.00727691	5	IFITM3
SERPINB4	2.44E-07	0.6142823	0.143	0.04	0.00755856	5	SERPINB4
CFD	2.48E-07	0.34704305	0.111	0.025	0.00769981	5	CFD
EFNA1	2.51E-07	0.42163656	0.201	0.073	0.00778308	5	EFNA1
S100A11	2.59E-07	0.50937282	0.429	0.235	0.00803668	5	S100A11
DHCR24	2.67E-07	0.31879544	0.122	0.031	0.00829295	5	DHCR24
MMP101	2.68E-07	0.80962131	0.201	0.09	0.0083277	5	MMP10
SERPINB9	3.47E-07	0.3212882	0.175	0.051	0.01077119	5	SERPINB9
CST3	3.55E-07	0.42047285	0.354	0.177	0.01100748	5	CST3
CPD	3.58E-07	0.31102776	0.101	0.023	0.01110115	5	CPD
CNN3	4.40E-07	0.48703854	0.159	0.051	0.01364744	5	CNN3
CEBD	7.33E-07	0.43794592	0.153	0.054	0.02274884	5	CEBD
NPM11	7.47E-07	0.36854305	0.429	0.235	0.02317338	5	NPM1
FOSB1	7.62E-07	0.31120141	0.725	0.536	0.02365522	5	FOSB
DST	8.27E-07	0.50139499	0.148	0.046	0.02565016	5	DST
ID2	8.88E-07	0.55877442	0.233	0.09	0.02756985	5	ID2
IER21	9.57E-07	0.34329902	0.566	0.361	0.02969632	5	IER2
ADAM152	1.06E-06	0.27092141	0.217	0.065	0.03301103	5	ADAM15
GAPDH1	1.13E-06	0.33416518	0.677	0.479	0.03506255	5	GAPDH
RND3	1.14E-06	0.4314324	0.111	0.025	0.03545303	5	RND3
GPX2	1.18E-06	0.37176333	0.106	0.025	0.03662632	5	GPX2
PTRF	1.20E-06	0.34136449	0.101	0.022	0.03734659	5	PTRF
SEPP1	1.25E-06	0.43681479	0.169	0.059	0.03887594	5	SEPP1

FTH1	1.33E-06	0.37552268	0.688	0.511	0.04138834	5	FTH1
MT-ND4	1.34E-06	0.41984365	0.603	0.408	0.0414458	5	MT-ND4
HPGD	1.34E-06	0.45629837	0.159	0.051	0.0414598	5	HPGD
APLP2	1.41E-06	0.46785662	0.275	0.117	0.04376661	5	APLP2
GSN	1.44E-06	0.5269002	0.175	0.06	0.04482473	5	GSN
IGHV1-184	7.58E-127	3.34675057	0.866	0.136	2.35E-122	6	IGHV1-18
IGHV1-83	1.54E-99	2.67863678	0.749	0.072	4.78E-95	6	IGHV1-8
IGKV3-205	6.37E-67	1.65398742	0.883	0.252	1.98E-62	6	IGKV3-20
IGHV1-23	1.91E-62	1.77913438	0.598	0.071	5.94E-58	6	IGHV1-2
IGKJ52	5.66E-59	1.9302788	0.615	0.127	1.76E-54	6	IGKJ5
IGHG44	6.92E-56	1.56052406	0.978	0.622	2.15E-51	6	IGHG4
IGKV3OR2-2683	4.91E-55	1.95140395	0.57	0.098	1.52E-50	6	IGKV3OR2-268
IGHV1-58	1.11E-48	1.93625591	0.397	0.033	3.44E-44	6	IGHV1-58
IGHV1-461	1.18E-43	1.95696647	0.464	0.058	3.67E-39	6	IGHV1-46
IGHV7-81	1.37E-43	2.03382025	0.341	0.026	4.25E-39	6	IGHV7-81
IGHV1OR15-12	3.27E-43	1.20661288	0.553	0.1	1.01E-38	6	IGHV1OR15-1
IGKV3D-205	8.52E-34	1.17797258	0.62	0.158	2.65E-29	6	IGKV3D-20
IGHG25	5.16E-31	0.48651714	0.95	0.526	1.60E-26	6	IGHG2
IGHV1OR15-9	1.03E-27	1.52681661	0.302	0.033	3.19E-23	6	IGHV1OR15-9
IGHV1-45	1.78E-25	1.41914287	0.335	0.062	5.51E-21	6	IGHV1-45
IGHV1-244	1.03E-22	2.48262137	0.503	0.21	3.19E-18	6	IGHV1-24
IGHV1-693	6.39E-20	0.93247048	0.536	0.17	1.98E-15	6	IGHV1-69
IGHV1OR21-1	4.54E-16	1.86822335	0.134	0.013	1.41E-11	6	IGHV1OR21-1
IGKV3D-112	6.28E-15	0.57636463	0.346	0.104	1.95E-10	6	IGKV3D-11
IGHV1-3	3.67E-13	1.83468538	0.179	0.036	1.14E-08	6	IGHV1-3
PFKL4	3.66E-12	0.5721708	0.358	0.141	1.14E-07	6	PFKL
IGHV6-11	5.79E-12	0.55108433	0.246	0.069	1.80E-07	6	IGHV6-1
POSTN3	3.04E-11	0.40843627	0.631	0.367	9.44E-07	6	POSTN
IGHE3	5.60E-11	0.60464395	0.24	0.07	1.74E-06	6	IGHE
IGKV3-73	2.24E-09	0.38266646	0.335	0.121	6.96E-05	6	IGKV3-7
IGKV3-15	1.23E-08	0.31370221	0.218	0.06	0.00038277	6	IGKV3-15
SNAP47	1.84E-07	0.48313408	0.184	0.064	0.00572271	6	SNAP47
BSG	1.24E-06	0.41470775	0.279	0.134	0.03846027	6	BSG
IGKV3-114	1.26E-32	2.59227565	0.585	0.175	3.92E-28	7	IGKV3-11
IGKV3-74	3.03E-32	1.72103464	0.507	0.113	9.40E-28	7	IGKV3-7
IGHV3-485	1.11E-28	1.79571325	0.563	0.142	3.46E-24	7	IGHV3-48
IGKV3D-113	4.13E-27	1.44222409	0.458	0.101	1.28E-22	7	IGKV3D-11
IGHV3-494	1.13E-26	1.82970703	0.444	0.088	3.49E-22	7	IGHV3-49
IGKV3D-15	2.78E-24	1.29132172	0.303	0.035	8.62E-20	7	IGKV3D-15

IGHV3-114	2.37E-23	2.07371366	0.472	0.121	7.37E-19	7	IGHV3-11
IGKV3D-206	7.74E-22	1.80001748	0.507	0.172	2.40E-17	7	IGKV3D-20
IGHV3-724	4.70E-18	0.99757165	0.359	0.074	1.46E-13	7	IGHV3-72
IGHV3OR16-9	9.84E-18	0.8407135	0.282	0.047	3.05E-13	7	IGHV3OR16-9
IGHV3OR16-125	2.34E-17	1.19625861	0.38	0.098	7.27E-13	7	IGHV3OR16-12
IGHV3-435	4.37E-17	1.18798319	0.493	0.154	1.35E-12	7	IGHV3-43
IGKV3D-72	2.28E-16	1.08365606	0.282	0.056	7.09E-12	7	IGKV3D-7
IGKV3-151	7.69E-16	2.31081051	0.275	0.059	2.39E-11	7	IGKV3-15
IGHV3OR15-71	2.84E-15	1.35890555	0.289	0.059	8.82E-11	7	IGHV3OR15-7
IGHV3-352	4.21E-15	1.18449272	0.261	0.046	1.31E-10	7	IGHV3-35
IGHV3OR16-81	3.76E-14	0.99316165	0.218	0.036	1.17E-09	7	IGHV3OR16-8
IGHV3-154	9.95E-14	2.2293058	0.352	0.119	3.09E-09	7	IGHV3-15
IGKV3OR2-2684	1.79E-12	0.74899867	0.38	0.118	5.57E-08	7	IGKV3OR2-268
IGHJ43	3.21E-12	1.26065804	0.415	0.182	9.97E-08	7	IGHJ4
IGHV3OR16-101	4.24E-11	0.72896469	0.246	0.058	1.31E-06	7	IGHV3OR16-10
IGKV2-28	5.61E-11	1.58667732	0.127	0.015	1.74E-06	7	IGKV2-28
IGKV2D-29	1.11E-10	1.36649449	0.127	0.014	3.45E-06	7	IGKV2D-29
IGHV3-215	2.59E-10	0.82800044	0.458	0.202	8.03E-06	7	IGHV3-21
IGKV2D-28	4.68E-10	1.19739867	0.113	0.012	1.45E-05	7	IGKV2D-28
IGKV3-206	9.76E-10	1.09370117	0.556	0.282	3.03E-05	7	IGKV3-20
IGHV3-744	3.19E-09	1.24641218	0.261	0.084	9.89E-05	7	IGHV3-74
IGHV3-203	3.54E-09	0.76250987	0.275	0.076	0.00010998	7	IGHV3-20
IGHV3-93	3.95E-09	0.55641497	0.303	0.104	0.00012248	7	IGHV3-9
IGKJ44	1.29E-08	1.59517143	0.331	0.141	0.00040184	7	IGKJ4
IGHV3-66	1.85E-08	0.91055683	0.134	0.023	0.00057416	7	IGHV3-66
IGHV3-531	2.17E-08	0.91537749	0.239	0.065	0.00067271	7	IGHV3-53
IGHV3-235	2.63E-08	0.59039877	0.521	0.238	0.00081509	7	IGHV3-23
IGHJ64	6.65E-08	0.8732615	0.331	0.155	0.00206376	7	IGHJ6
IGHV3-645	2.61E-07	0.9574306	0.275	0.102	0.00810125	7	IGHV3-64
IGHV3-131	6.78E-07	2.24765121	0.225	0.077	0.02102905	7	IGHV3-13
IGHV3-77	8.18E-07	1.16218074	0.261	0.101	0.02538731	7	IGHV3-7
AC096579.75	1.05E-06	0.91409858	0.739	0.561	0.03247388	7	AC096579.7
HIST1H2AJ	1.42E-42	1.36442297	0.419	0.006	4.40E-38	8	HIST1H2AJ
HIST1H1B	5.33E-42	1.8046723	0.419	0.01	1.66E-37	8	HIST1H1B
HIST1H4C2	2.95E-40	2.00712987	0.763	0.233	9.16E-36	8	HIST1H4C
STMN1	2.29E-39	1.21552058	0.495	0.025	7.11E-35	8	STMN1

MKI67	1.46E-38	1.04957321	0.43	0.008	4.55E-34	8	MKI67
RRM2	3.85E-37	1.08303031	0.376	0.006	1.20E-32	8	RRM2
HMGB2	4.47E-37	1.48579432	0.699	0.098	1.39E-32	8	HMGB2
TUBA1B	5.36E-37	1.51788775	0.753	0.16	1.66E-32	8	TUBA1B
PTMA	1.84E-36	1.28760844	0.957	0.542	5.71E-32	8	PTMA
H2AFZ	1.22E-35	1.37025197	0.849	0.274	3.78E-31	8	H2AFZ
SHCBP1	8.77E-35	0.98617885	0.419	0.01	2.72E-30	8	SHCBP1
PPIB2	1.35E-34	1.12258176	0.989	0.631	4.20E-30	8	PPIB
GGH	1.96E-34	1.23057709	0.645	0.073	6.07E-30	8	GGH
BIRC5	2.47E-33	0.95922981	0.387	0.005	7.68E-29	8	BIRC5
GAPDH2	4.82E-32	1.22417918	0.925	0.478	1.49E-27	8	GAPDH
RPS24	1.23E-31	1.07225658	0.978	0.721	3.82E-27	8	RPS24
RAN1	1.69E-30	1.17616827	0.796	0.202	5.24E-26	8	RAN
PTTG1	2.08E-29	1.17856965	0.43	0.027	6.45E-25	8	PTTG1
CENPW	1.40E-27	0.9742337	0.333	0.009	4.34E-23	8	CENPW
HIST1H1C2	5.83E-27	1.2895416	0.72	0.168	1.81E-22	8	HIST1H1C
CHCHD21	1.28E-25	1.00644135	0.892	0.41	3.99E-21	8	CHCHD2
KIAA0101	2.08E-25	1.01818558	0.333	0.009	6.46E-21	8	KIAA0101
SMC4	6.76E-25	1.12282549	0.538	0.075	2.10E-20	8	SMC4
TYMS	9.21E-25	0.9393994	0.301	0.009	2.86E-20	8	TYMS
DUT1	2.16E-24	1.08448316	0.516	0.087	6.71E-20	8	DUT
CCT2	2.48E-24	0.87629749	0.484	0.051	7.69E-20	8	CCT2
UQCRH1	5.16E-24	0.95207044	0.892	0.373	1.60E-19	8	UQCRH
HMGB1	1.65E-23	1.15566612	0.731	0.276	5.11E-19	8	HMGB1
COX8A	2.09E-23	0.97594538	0.796	0.279	6.48E-19	8	COX8A
DLGAP5	7.39E-23	0.60786778	0.215	0.003	2.29E-18	8	DLGAP5
SUB1	4.17E-22	0.8798025	0.968	0.643	1.29E-17	8	SUB1
NPM12	5.71E-22	1.06183419	0.71	0.232	1.77E-17	8	NPM1
RPS21	9.02E-22	0.74297849	1	0.843	2.80E-17	8	RPS21
RPS19	1.03E-21	0.65507605	1	0.957	3.19E-17	8	RPS19
C1QBP	1.83E-21	0.96445434	0.667	0.177	5.67E-17	8	C1QBP
TUBB	2.01E-21	1.01186028	0.462	0.054	6.25E-17	8	TUBB
SNRPB	7.14E-21	0.98677242	0.591	0.12	2.22E-16	8	SNRPB
C19orf101	9.38E-21	0.87605114	0.892	0.543	2.91E-16	8	C19orf10
PPIA2	1.11E-20	1.06370409	0.613	0.172	3.44E-16	8	PPIA
ATP5G31	5.26E-20	0.84671902	0.871	0.347	1.63E-15	8	ATP5G3
NUSAP1	5.64E-20	0.74758698	0.247	0.008	1.75E-15	8	NUSAP1
TPX2	1.08E-19	0.67229973	0.226	0.004	3.35E-15	8	TPX2
MAD2L1	1.19E-19	0.82759151	0.258	0.008	3.70E-15	8	MAD2L1
LDHA	1.22E-19	0.90556165	0.72	0.229	3.77E-15	8	LDHA

PSME21	2.20E-19	0.90539267	0.731	0.279	6.84E-15	8	PSME2
ASPM	4.47E-19	0.65863263	0.226	0.006	1.39E-14	8	ASPM
SLC25A5	8.27E-19	0.83094834	0.699	0.215	2.57E-14	8	SLC25A5
NME11	1.23E-18	0.90083758	0.699	0.21	3.83E-14	8	NME1
RPL35	1.58E-18	0.70014485	0.978	0.882	4.89E-14	8	RPL35
PA2G4	1.86E-18	0.90214904	0.538	0.1	5.78E-14	8	PA2G4
RPL19	2.39E-18	0.61885172	1	0.869	7.40E-14	8	RPL19
CENPN	2.42E-18	0.71140835	0.28	0.01	7.52E-14	8	CENPN
RPS7	2.51E-18	0.80501634	0.882	0.551	7.78E-14	8	RPS7
SNRPD2	3.71E-18	0.82908728	0.817	0.334	1.15E-13	8	SNRPD2
NDUFB6	4.31E-18	0.8923506	0.742	0.258	1.34E-13	8	NDUFB6
RPS13	5.31E-18	0.65054451	1	0.845	1.65E-13	8	RPS13
HNRNPA2B12	5.42E-18	0.76747474	0.871	0.407	1.68E-13	8	HNRNPA2B1
EBNA1BP2	5.87E-18	0.84299288	0.441	0.078	1.82E-13	8	EBNA1BP2
CENPE	6.17E-18	0.60660149	0.183	0.004	1.91E-13	8	CENPE
EIF5A	6.60E-18	0.85222438	0.688	0.212	2.05E-13	8	EIF5A
TMPO	8.56E-18	0.89149681	0.484	0.081	2.66E-13	8	TMPO
TOP2A	9.83E-18	0.59092447	0.237	0.008	3.05E-13	8	TOP2A
HMGN2	1.49E-17	0.94193332	0.441	0.079	4.61E-13	8	HMGN2
PFN1	1.70E-17	0.87039996	0.731	0.279	5.28E-13	8	PFN1
COX6A1	2.22E-17	0.79434649	0.817	0.397	6.89E-13	8	COX6A1
RPS16	2.44E-17	0.62104246	1	0.86	7.57E-13	8	RPS16
TPI1	2.49E-17	0.90330203	0.656	0.227	7.72E-13	8	TPI1
COX6B1	4.00E-17	0.85082133	0.796	0.369	1.24E-12	8	COX6B1
PBK	4.76E-17	0.49931644	0.151	0.001	1.48E-12	8	PBK
ENO1	5.22E-17	0.82714414	0.688	0.225	1.62E-12	8	ENO1
ATP5E	6.94E-17	0.66662443	0.946	0.587	2.15E-12	8	ATP5E
YBX12	6.99E-17	0.85162567	0.731	0.291	2.17E-12	8	YBX1
ARPC3	8.45E-17	0.75705669	0.72	0.219	2.62E-12	8	ARPC3
TROAP	1.36E-16	0.5313581	0.204	0.004	4.23E-12	8	TROAP
CD52	2.53E-16	0.99995337	0.645	0.155	7.85E-12	8	CD52
CCNA2	3.83E-16	0.67570452	0.172	0.003	1.19E-11	8	CCNA2
CYCS	4.46E-16	0.82387035	0.656	0.208	1.38E-11	8	CYCS
MLF1IP	4.87E-16	0.54544513	0.237	0.01	1.51E-11	8	MLF1IP
MRPS34	7.44E-16	0.80900815	0.591	0.153	2.31E-11	8	MRPS34
RPL27	8.06E-16	0.59594727	0.989	0.867	2.50E-11	8	RPL27
PSMB3	8.88E-16	0.75625754	0.688	0.214	2.76E-11	8	PSMB3
ACTB1	1.51E-15	0.76689177	0.774	0.331	4.70E-11	8	ACTB
ATP5G1	2.27E-15	0.80644056	0.699	0.243	7.06E-11	8	ATP5G1
PSMA6	2.46E-15	0.84586612	0.677	0.23	7.64E-11	8	PSMA6

TK1	2.48E-15	0.49922222	0.183	0.005	7.70E-11	8	TK1
RPS18	2.48E-15	0.55080366	1	0.969	7.71E-11	8	RPS18
HMGA1	2.66E-15	0.83417677	0.387	0.065	8.25E-11	8	HMGA1
COX6C	3.01E-15	0.71977827	0.796	0.376	9.34E-11	8	COX6C
CDK1	3.54E-15	0.65018382	0.204	0.009	1.10E-10	8	CDK1
RPL10A1	4.26E-15	0.63077791	0.957	0.607	1.32E-10	8	RPL10A
NCL	4.88E-15	0.68414627	0.796	0.343	1.52E-10	8	NCL
RPL51	4.91E-15	0.65296383	0.989	0.695	1.52E-10	8	RPL5
UBA52	5.66E-15	0.70273278	0.882	0.549	1.76E-10	8	UBA52
RPS25	5.69E-15	0.59871438	0.968	0.765	1.77E-10	8	RPS25
HNRNPM1	5.79E-15	0.70683201	0.57	0.137	1.80E-10	8	HNRNPM
HSP90B11	6.17E-15	0.61467796	0.989	0.928	1.91E-10	8	HSP90B1
ANP32B	6.97E-15	0.88226075	0.527	0.13	2.16E-10	8	ANP32B
RPS15	7.31E-15	0.62738401	0.957	0.701	2.27E-10	8	RPS15
PSMD8	8.83E-15	0.74879607	0.667	0.193	2.74E-10	8	PSMD8
RPL24	8.92E-15	0.63202037	0.946	0.69	2.77E-10	8	RPL24
SKA1	1.17E-14	0.32225926	0.118	0	3.64E-10	8	SKA1
RPL411	1.39E-14	0.62970321	0.968	0.872	4.32E-10	8	RPL41
RBM3	1.46E-14	0.72175827	0.839	0.378	4.53E-10	8	RBM3
RPL22L1	1.72E-14	0.65550611	0.806	0.312	5.34E-10	8	RPL22L1
TIMM8B	1.73E-14	0.75227535	0.516	0.114	5.36E-10	8	TIMM8B
EIF3I	2.11E-14	0.65737326	0.591	0.158	6.54E-10	8	EIF3I
COX7B	2.14E-14	0.72123962	0.742	0.313	6.65E-10	8	COX7B
RPS8	2.31E-14	0.47784843	1	0.957	7.18E-10	8	RPS8
SERF2	2.51E-14	0.62292728	0.935	0.748	7.79E-10	8	SERF2
SSR3	2.66E-14	0.62372747	0.957	0.704	8.25E-10	8	SSR3
NDUFA6	2.74E-14	0.72990864	0.72	0.273	8.51E-10	8	NDUFA6
TMSB4X2	3.08E-14	0.69119101	0.935	0.633	9.55E-10	8	TMSB4X
SERBP1	3.67E-14	0.663449	0.667	0.227	1.14E-09	8	SERBP1
LSMD1	4.41E-14	0.74258783	0.667	0.209	1.37E-09	8	LSMD1
SNRPG	5.46E-14	0.71917134	0.505	0.126	1.70E-09	8	SNRPG
LSM7	5.55E-14	0.74114071	0.591	0.153	1.72E-09	8	LSM7
DTYMK	5.65E-14	0.68237513	0.269	0.025	1.75E-09	8	DTYMK
TRIP13	6.02E-14	0.49996628	0.172	0.004	1.87E-09	8	TRIP13
ZWINT	7.01E-14	0.44095075	0.14	0.003	2.17E-09	8	ZWINT
IDH2	7.21E-14	0.81595042	0.559	0.177	2.24E-09	8	IDH2
HSPD11	7.84E-14	0.76194331	0.613	0.203	2.43E-09	8	HSPD1
UQCR10	7.99E-14	0.684376	0.656	0.234	2.48E-09	8	UQCR10
CCND24	8.13E-14	0.74301466	0.828	0.421	2.52E-09	8	CCND2
SET1	8.45E-14	0.63384915	0.548	0.147	2.62E-09	8	SET

RPL14	9.29E-14	0.60933473	0.914	0.628	2.88E-09	8	RPL14
MCM4	1.07E-13	0.52152298	0.204	0.013	3.33E-09	8	MCM4
MRPL22	1.09E-13	0.72728413	0.462	0.09	3.37E-09	8	MRPL22
RPS6	1.24E-13	0.44311667	1	0.984	3.83E-09	8	RPS6
NDUFA41	1.32E-13	0.58410788	0.935	0.629	4.09E-09	8	NDUFA4
FANCI	1.54E-13	0.55923814	0.226	0.009	4.78E-09	8	FANCI
CORO1A	1.65E-13	0.6873761	0.366	0.049	5.13E-09	8	CORO1A
SEC61B1	1.71E-13	0.62129564	0.903	0.608	5.30E-09	8	SEC61B
RPS2	1.79E-13	0.75490386	0.828	0.481	5.56E-09	8	RPS2
SNRPF	1.95E-13	0.73498469	0.376	0.064	6.06E-09	8	SNRPF
CALR	1.99E-13	0.60366036	0.903	0.522	6.16E-09	8	CALR
RPL36AL1	2.14E-13	0.61998212	0.914	0.594	6.63E-09	8	RPL36AL
RPL29	2.90E-13	0.62616001	0.828	0.435	9.00E-09	8	RPL29
COX7A21	2.90E-13	0.60162323	0.925	0.613	9.00E-09	8	COX7A2
CBX3	2.99E-13	0.72083122	0.548	0.135	9.29E-09	8	CBX3
ATP5J2	3.22E-13	0.77315057	0.613	0.214	9.99E-09	8	ATP5J2
UQCRQ	3.23E-13	0.65673168	0.882	0.588	1.00E-08	8	UQCRQ
P4HB	3.87E-13	0.65081903	0.806	0.411	1.20E-08	8	P4HB
SDF2L11	5.10E-13	0.67037066	0.806	0.395	1.58E-08	8	SDF2L1
OSTC	5.65E-13	0.67041079	0.806	0.409	1.75E-08	8	OSTC
RPL282	6.69E-13	0.63860804	0.849	0.468	2.08E-08	8	RPL28
RPL37A	1.01E-12	0.53813164	0.968	0.825	3.14E-08	8	RPL37A
TMEM106C	1.04E-12	0.63528049	0.333	0.039	3.21E-08	8	TMEM106C
MIF	1.05E-12	0.65866017	0.806	0.434	3.25E-08	8	MIF
LDHB1	1.06E-12	0.75737063	0.516	0.158	3.30E-08	8	LDHB
DHFR	1.35E-12	0.45246989	0.14	0.003	4.20E-08	8	DHFR
SNRPE1	1.51E-12	0.69528314	0.409	0.089	4.69E-08	8	SNRPE
RPS15A	1.69E-12	0.52823397	0.978	0.851	5.24E-08	8	RPS15A
C14orf2	1.73E-12	0.64177449	0.731	0.312	5.37E-08	8	C14orf2
NOP10	1.85E-12	0.66708916	0.527	0.146	5.75E-08	8	NOP10
SSBP1	1.88E-12	0.58380862	0.57	0.141	5.84E-08	8	SSBP1
C19orf48	1.89E-12	0.45678614	0.258	0.021	5.86E-08	8	C19orf48
RPL8	1.91E-12	0.51694027	0.968	0.801	5.92E-08	8	RPL8
COPE	1.95E-12	0.63112724	0.731	0.313	6.05E-08	8	COPE
PDCD5	2.01E-12	0.66604371	0.484	0.113	6.23E-08	8	PDCD5
SEC61G	2.03E-12	0.58315885	0.86	0.427	6.31E-08	8	SEC61G
SDHB	2.25E-12	0.6113562	0.452	0.089	6.99E-08	8	SDHB
CYC11	2.43E-12	0.65290793	0.581	0.163	7.55E-08	8	CYC1
HMMR	2.45E-12	0.53101531	0.161	0.009	7.62E-08	8	HMMR
PDIA6	2.58E-12	0.59992175	0.925	0.639	8.01E-08	8	PDIA6

SGOL1	2.77E-12	0.25127857	0.108	0.001	8.59E-08	8	SGOL1
CDKN3	2.88E-12	0.88704749	0.215	0.009	8.94E-08	8	CDKN3
RPL32	3.03E-12	0.53212877	0.978	0.817	9.40E-08	8	RPL32
PPA1	3.35E-12	0.6590786	0.591	0.183	1.04E-07	8	PPA1
MZB12	3.63E-12	0.49111111	1	0.901	1.13E-07	8	MZB1
KIF11	4.26E-12	0.41965462	0.151	0.005	1.32E-07	8	KIF11
TMSB103	4.39E-12	0.63038738	0.957	0.69	1.36E-07	8	TMSB10
SF3B52	4.64E-12	0.64477132	0.624	0.206	1.44E-07	8	SF3B5
LSM3	4.86E-12	0.77719568	0.591	0.185	1.51E-07	8	LSM3
ATP5C1	5.05E-12	0.61389553	0.591	0.17	1.57E-07	8	ATP5C1
ANP32E	5.16E-12	0.59444394	0.419	0.089	1.60E-07	8	ANP32E
CDCA3	6.51E-12	0.58185996	0.161	0.003	2.02E-07	8	CDCA3
MRPL27	6.76E-12	0.65182788	0.344	0.054	2.10E-07	8	MRPL27
MYL6	6.81E-12	0.50199854	0.968	0.687	2.11E-07	8	MYL6
EIF2S1	7.02E-12	0.75876246	0.409	0.082	2.18E-07	8	EIF2S1
FAU1	7.81E-12	0.44854763	0.989	0.88	2.42E-07	8	FAU
PSMB61	9.20E-12	0.64555236	0.613	0.23	2.85E-07	8	PSMB6
HIST1H1E	9.24E-12	0.78447102	0.387	0.08	2.87E-07	8	HIST1H1E
CDC6	9.53E-12	0.63489755	0.226	0.022	2.96E-07	8	CDC6
PFDN4	1.06E-11	0.608435	0.355	0.058	3.28E-07	8	PFDN4
PRELID1	1.12E-11	0.659233	0.624	0.244	3.49E-07	8	PRELID1
HSPE1	1.14E-11	0.57881458	0.57	0.154	3.53E-07	8	HSPE1
ATP5L	1.15E-11	0.64439956	0.839	0.494	3.58E-07	8	ATP5L
ARPC2	1.21E-11	0.58638185	0.806	0.413	3.74E-07	8	ARPC2
NDUFB4	1.31E-11	0.68251808	0.656	0.255	4.05E-07	8	NDUFB4
NDUFS51	1.31E-11	0.69775334	0.591	0.21	4.06E-07	8	NDUFS5
RPL35A1	1.32E-11	0.46085528	1	0.905	4.10E-07	8	RPL35A
UBE2C	1.36E-11	0.446694	0.14	0.003	4.23E-07	8	UBE2C
HIST1H2AH	1.49E-11	0.46591203	0.183	0.009	4.62E-07	8	HIST1H2AH
HIST1H2BM	1.50E-11	0.48836063	0.129	0.002	4.67E-07	8	HIST1H2BM
ERH	1.63E-11	0.66200181	0.613	0.211	5.05E-07	8	ERH
CD320	1.66E-11	0.60101572	0.387	0.067	5.14E-07	8	CD320
NOP581	1.85E-11	0.60562199	0.613	0.197	5.74E-07	8	NOP58
RPL15	1.92E-11	0.46861329	0.978	0.866	5.95E-07	8	RPL15
PAICS	1.92E-11	0.61845489	0.323	0.054	5.95E-07	8	PAICS
PSMB1	1.95E-11	0.56178893	0.753	0.311	6.04E-07	8	PSMB1
RPL11	1.96E-11	0.47101415	0.989	0.897	6.09E-07	8	RPL11
NCAPG	1.99E-11	0.41131751	0.118	0.004	6.17E-07	8	NCAPG
XRCC5	2.10E-11	0.60755994	0.516	0.161	6.52E-07	8	XRCC5
RPS11	2.10E-11	0.40622191	1	0.897	6.53E-07	8	RPS11

NDUFB1	2.22E-11	0.66269157	0.699	0.295	6.90E-07	8	NDUFB1
HNRNPA11	2.30E-11	0.64497454	0.581	0.195	7.15E-07	8	HNRNPA11
ATP5J	2.34E-11	0.63830883	0.731	0.352	7.27E-07	8	ATP5J
PSMA4	2.36E-11	0.62101099	0.495	0.135	7.31E-07	8	PSMA4
RACGAP1	2.43E-11	0.35229333	0.151	0.003	7.53E-07	8	RACGAP1
KIF20B	2.67E-11	0.46660947	0.226	0.021	8.29E-07	8	KIF20B
SRP14	2.85E-11	0.60729602	0.71	0.291	8.86E-07	8	SRP14
PET100	3.04E-11	0.64385128	0.548	0.18	9.42E-07	8	PET100
LRRC59	3.14E-11	0.67829049	0.516	0.165	9.75E-07	8	LRRC59
CAPZA1	3.20E-11	0.64289505	0.548	0.163	9.92E-07	8	CAPZA1
CBX5	3.21E-11	0.60034025	0.323	0.057	9.96E-07	8	CBX5
CD99	3.23E-11	0.60620352	0.516	0.156	1.00E-06	8	CD99
RPS121	3.30E-11	0.45093355	0.989	0.908	1.02E-06	8	RPS12
AP2S1	3.37E-11	0.64191235	0.409	0.094	1.04E-06	8	AP2S1
C12orf75	3.39E-11	0.64741041	0.247	0.028	1.05E-06	8	C12orf75
MRPL52	3.60E-11	0.6753285	0.57	0.197	1.12E-06	8	MRPL52
RPL37	3.74E-11	0.53253868	0.946	0.702	1.16E-06	8	RPL37
CKS2	4.16E-11	0.72889262	0.462	0.1	1.29E-06	8	CKS2
XRCC6	4.26E-11	0.69222437	0.516	0.133	1.32E-06	8	XRCC6
SNRNP25	4.72E-11	0.71319272	0.323	0.052	1.47E-06	8	SNRNP25
TKT1	4.77E-11	0.58554722	0.43	0.107	1.48E-06	8	TKT
IFI30	4.93E-11	0.63204355	0.527	0.157	1.53E-06	8	IFI30
MLEC1	4.94E-11	0.66669009	0.581	0.188	1.53E-06	8	MLEC
HNRNPK	5.85E-11	0.53751825	0.677	0.264	1.82E-06	8	HNRNPK
TXN1	5.98E-11	0.68406374	0.688	0.34	1.86E-06	8	TXN
RPL30	6.02E-11	0.42754063	0.978	0.866	1.87E-06	8	RPL30
UBE2T	6.28E-11	0.40877891	0.183	0.015	1.95E-06	8	UBE2T
NDUFS7	6.42E-11	0.64455817	0.505	0.156	1.99E-06	8	NDUFS7
ATP5I	6.47E-11	0.553983	0.753	0.361	2.01E-06	8	ATP5I
OST4	6.57E-11	0.53333443	0.914	0.573	2.04E-06	8	OST4
HIST1H1D	6.60E-11	0.83144458	0.333	0.075	2.05E-06	8	HIST1H1D
RPN2	7.30E-11	0.55955607	0.892	0.544	2.27E-06	8	RPN2
HNRNPC	7.42E-11	0.69491443	0.505	0.171	2.30E-06	8	HNRNPC
SRP72	7.50E-11	0.59004112	0.656	0.247	2.33E-06	8	SRP72
TRMT112	9.18E-11	0.56941697	0.71	0.305	2.85E-06	8	TRMT112
ATP5F1	9.34E-11	0.63017827	0.505	0.164	2.90E-06	8	ATP5F1
BTF31	1.01E-10	0.56112731	0.753	0.369	3.12E-06	8	BTF3
YWHAE	1.03E-10	0.60594385	0.645	0.26	3.19E-06	8	YWHAE
H2AFV	1.04E-10	0.53815097	0.409	0.088	3.22E-06	8	H2AFV
MTDH2	1.09E-10	0.446683	0.839	0.453	3.39E-06	8	MTDH2

CACYBP	1.17E-10	0.71737682	0.387	0.076	3.62E-06	8	CACYBP
ATP5O	1.19E-10	0.64177654	0.634	0.254	3.70E-06	8	ATP5O
SNRPC	1.25E-10	0.58432268	0.495	0.126	3.86E-06	8	SNRPC
POMP	1.26E-10	0.62242695	0.581	0.203	3.92E-06	8	POMP
MRPS14	1.43E-10	0.58052194	0.398	0.081	4.43E-06	8	MRPS14
HNRNPR	1.51E-10	0.55896354	0.484	0.139	4.69E-06	8	HNRNPR
CLPP	1.66E-10	0.57319846	0.376	0.074	5.15E-06	8	CLPP
NDUFA11	1.68E-10	0.53164406	0.774	0.375	5.20E-06	8	NDUFA11
SPC25	1.69E-10	0.44231682	0.161	0.004	5.24E-06	8	SPC25
ATP5G2	1.75E-10	0.56018773	0.72	0.342	5.43E-06	8	ATP5G2
TCEB2	1.81E-10	0.51893635	0.763	0.357	5.62E-06	8	TCEB2
RPL31	2.02E-10	0.45512797	0.978	0.845	6.26E-06	8	RPL31
RPL26	2.23E-10	0.48569098	0.935	0.718	6.91E-06	8	RPL26
SRSF3	2.24E-10	0.58290955	0.656	0.261	6.94E-06	8	SRSF3
RPL13	2.49E-10	0.3852479	1	0.955	7.72E-06	8	RPL13
SSR2	2.59E-10	0.56931221	0.796	0.445	8.04E-06	8	SSR2
MELK	2.64E-10	0.37246459	0.14	0.003	8.20E-06	8	MELK
MCM3	2.76E-10	0.4095223	0.194	0.015	8.58E-06	8	MCM3
SMC2	2.77E-10	0.53749251	0.215	0.021	8.61E-06	8	SMC2
ATP5EP2	2.83E-10	0.67406484	0.484	0.124	8.78E-06	8	ATP5EP2
DDX39A	2.94E-10	0.59128457	0.398	0.076	9.11E-06	8	DDX39A
PSME1	2.98E-10	0.54441653	0.753	0.386	9.25E-06	8	PSME1
CEP55	2.99E-10	0.34030054	0.118	0.002	9.27E-06	8	CEP55
HNRNPAB	3.07E-10	0.61780977	0.333	0.064	9.51E-06	8	HNRNPAB
MDH21	3.14E-10	0.59925177	0.462	0.117	9.75E-06	8	MDH2
CCT4	3.31E-10	0.58045391	0.387	0.086	1.03E-05	8	CCT4
HIST1H2AM	3.37E-10	0.38711087	0.161	0.006	1.04E-05	8	HIST1H2AM
MCM7	3.42E-10	0.44087695	0.215	0.019	1.06E-05	8	MCM7
COX5B1	3.45E-10	0.57120456	0.731	0.346	1.07E-05	8	COX5B
BUB1	3.47E-10	0.42673613	0.151	0.008	1.08E-05	8	BUB1
RPS5	3.55E-10	0.40680681	1	0.853	1.10E-05	8	RPS5
GTF3A5	3.57E-10	0.56385081	0.72	0.348	1.11E-05	8	GTF3A
PSMA3	3.76E-10	0.58887993	0.538	0.176	1.17E-05	8	PSMA3
PDIA41	3.78E-10	0.53677155	0.796	0.47	1.17E-05	8	PDIA4
RPL23A	4.04E-10	0.4712607	0.892	0.559	1.25E-05	8	RPL23A
ACAT2	4.13E-10	0.47171721	0.204	0.022	1.28E-05	8	ACAT2
RPS9	4.27E-10	0.42554797	0.978	0.776	1.32E-05	8	RPS9
BCCIP	4.39E-10	0.64638285	0.366	0.064	1.36E-05	8	BCCIP
FBL	4.41E-10	0.6216618	0.376	0.086	1.37E-05	8	FBL
CCT6A	4.47E-10	0.58478206	0.398	0.099	1.39E-05	8	CCT6A

ARHGDI1B	4.48E-10	0.56765149	0.591	0.231	1.39E-05	8	ARHGDI1B
DIAPH3	5.16E-10	0.43283872	0.108	0.004	1.60E-05	8	DIAPH3
MRPL12	5.16E-10	0.49004285	0.387	0.07	1.60E-05	8	MRPL12
RPS27A	5.38E-10	0.44364163	0.978	0.872	1.67E-05	8	RPS27A
MZT2B	5.57E-10	0.61113273	0.452	0.124	1.73E-05	8	MZT2B
RPS23	5.58E-10	0.49073233	0.946	0.753	1.73E-05	8	RPS23
NACA	5.63E-10	0.5303969	0.839	0.528	1.75E-05	8	NACA
NDUFA1	5.71E-10	0.51779743	0.839	0.473	1.77E-05	8	NDUFA1
RPLP0	6.01E-10	0.40486856	1	0.939	1.86E-05	8	RPLP0
MINOS1	6.55E-10	0.63486225	0.419	0.104	2.03E-05	8	MINOS1
NDC80	6.82E-10	0.32336837	0.14	0.004	2.12E-05	8	NDC80
PSMA7	6.92E-10	0.57439804	0.645	0.291	2.15E-05	8	PSMA7
HINT1	7.17E-10	0.47758356	0.892	0.525	2.22E-05	8	HINT1
CEP57	7.19E-10	0.61852974	0.355	0.065	2.23E-05	8	CEP57
PSMA5	7.25E-10	0.57889671	0.441	0.112	2.25E-05	8	PSMA5
RPL4	7.29E-10	0.52062581	0.903	0.687	2.26E-05	8	RPL4
YWHAZ	7.84E-10	0.55578626	0.624	0.232	2.43E-05	8	YWHAZ
RABAC1	7.86E-10	0.52783977	0.817	0.454	2.44E-05	8	RABAC1
RRM1	7.90E-10	0.60931512	0.183	0.015	2.45E-05	8	RRM1
LYAR	8.60E-10	0.47626922	0.215	0.025	2.67E-05	8	LYAR
RPS31	8.69E-10	0.50460902	0.935	0.767	2.70E-05	8	RPS3
BRCA1	8.84E-10	0.33091468	0.118	0.006	2.74E-05	8	BRCA1
COX5A1	9.39E-10	0.48046889	0.72	0.339	2.91E-05	8	COX5A
HSPA5	9.53E-10	0.57323492	0.946	0.703	2.96E-05	8	HSPA5
HMGN1	1.04E-09	0.67469716	0.505	0.165	3.22E-05	8	HMGN1
HJURP	1.17E-09	0.30522611	0.118	0.001	3.64E-05	8	HJURP
CDC20	1.41E-09	0.32552667	0.108	0.002	4.37E-05	8	CDC20
ATP5H	1.46E-09	0.47205269	0.548	0.182	4.53E-05	8	ATP5H
RPN1	1.49E-09	0.53895115	0.753	0.377	4.63E-05	8	RPN1
TAGLN2	1.52E-09	0.60575433	0.505	0.167	4.71E-05	8	TAGLN2
PARPBP	1.54E-09	0.38174133	0.129	0.007	4.78E-05	8	PARPBP
MRP63	1.54E-09	0.5230303	0.57	0.176	4.79E-05	8	MRP63
ANAPC11	1.55E-09	0.50141749	0.677	0.301	4.81E-05	8	ANAPC11
ATAD2	1.59E-09	0.4564501	0.161	0.011	4.94E-05	8	ATAD2
PSMB7	1.64E-09	0.63343449	0.505	0.153	5.10E-05	8	PSMB7
RPL23	1.74E-09	0.48438944	0.892	0.62	5.40E-05	8	RPL23
POLR2E	1.77E-09	0.53254695	0.355	0.074	5.50E-05	8	POLR2E
POLR2L	1.81E-09	0.53354649	0.688	0.311	5.62E-05	8	POLR2L
EDEM1	1.86E-09	0.53689113	0.505	0.155	5.78E-05	8	EDEM1
LGALS11	1.90E-09	0.63479644	0.731	0.418	5.90E-05	8	LGALS11

ACAT1	1.97E-09	0.4919894	0.43	0.092	6.13E-05	8	ACAT1
RPL211	2.02E-09	0.51396847	0.688	0.32	6.26E-05	8	RPL21
PPM1G	2.10E-09	0.65205154	0.419	0.12	6.52E-05	8	PPM1G
RPS4X	2.12E-09	0.3990374	1	0.872	6.58E-05	8	RPS4X
NOP56	2.26E-09	0.53386434	0.419	0.113	7.03E-05	8	NOP56
PRDX31	2.34E-09	0.56433243	0.484	0.129	7.27E-05	8	PRDX3
COX4I1	2.52E-09	0.47167539	0.86	0.555	7.82E-05	8	COX4I1
RPL18	2.67E-09	0.44356365	0.935	0.707	8.29E-05	8	RPL18
DDOST	2.67E-09	0.53485044	0.688	0.316	8.29E-05	8	DDOST
ESCO2	2.71E-09	0.28117825	0.118	0.001	8.40E-05	8	ESCO2
PGK1	3.07E-09	0.54236091	0.581	0.218	9.54E-05	8	PGK1
HIST2H2AC	3.22E-09	0.48195836	0.226	0.028	9.99E-05	8	HIST2H2AC
RPL361	3.24E-09	0.49138517	0.892	0.638	0.00010064	8	RPL36
PRR11	3.30E-09	0.30737367	0.118	0.003	0.00010236	8	PRR11
FEN1	3.45E-09	0.53052034	0.237	0.029	0.00010712	8	FEN1
DDX21	3.53E-09	0.5381209	0.398	0.093	0.00010954	8	DDX21
RPS27L	3.54E-09	0.42802017	0.774	0.402	0.00010979	8	RPS27L
APOBEC3B	3.60E-09	0.48868571	0.215	0.025	0.00011159	8	APOBEC3B
POLQ	3.63E-09	0.35262098	0.129	0.004	0.00011263	8	POLQ
CALM3	3.65E-09	0.541434	0.441	0.097	0.00011319	8	CALM3
TMED91	4.26E-09	0.47318948	0.774	0.39	0.00013225	8	TMED9
RBX11	4.44E-09	0.50459969	0.548	0.194	0.00013781	8	RBX1
LRPAP1	4.51E-09	0.52603445	0.57	0.205	0.00013994	8	LRPAP1
PRIM1	4.80E-09	0.36192104	0.161	0.018	0.0001489	8	PRIM1
ATP5A1	4.98E-09	0.50844061	0.72	0.345	0.00015452	8	ATP5A1
RPL38	5.14E-09	0.49432951	0.839	0.623	0.0001595	8	RPL38
RPS291	5.20E-09	0.39284176	0.968	0.921	0.0001613	8	RPS29
LMAN1	5.39E-09	0.55288609	0.806	0.469	0.00016729	8	LMAN1
HIST1H2AG	5.41E-09	0.33713958	0.172	0.018	0.00016792	8	HIST1H2AG
TPM3	5.72E-09	0.78018729	0.441	0.16	0.00017748	8	TPM3
MANF	5.85E-09	0.49772964	0.774	0.406	0.00018165	8	MANF
HIST1H4E	5.93E-09	0.4292257	0.151	0.01	0.00018391	8	HIST1H4E
ACTG11	6.00E-09	0.69726316	0.731	0.427	0.00018604	8	ACTG1
CENPF	6.00E-09	0.355097	0.108	0.006	0.00018614	8	CENPF
LMAN2	6.24E-09	0.46137836	0.731	0.375	0.00019355	8	LMAN2
HSP90AA11	6.42E-09	0.53948854	0.688	0.301	0.00019915	8	HSP90AA1
PSMB2	6.79E-09	0.48550065	0.473	0.121	0.00021081	8	PSMB2
KPNA2	6.91E-09	0.49809821	0.194	0.024	0.00021452	8	KPNA2
MYEOV2	7.18E-09	0.4745935	0.548	0.201	0.00022284	8	MYEOV2
COX17	7.19E-09	0.51027824	0.505	0.17	0.00022312	8	COX17

SNRPD1	7.47E-09	0.5190397	0.355	0.105	0.00023166	8	SNRPD1
CTPS1	7.57E-09	0.32360961	0.14	0.008	0.00023482	8	CTPS1
NDUFAB11	7.74E-09	0.45395364	0.559	0.202	0.00024032	8	NDUFAB11
ANP32A	7.82E-09	0.38573401	0.28	0.053	0.00024261	8	ANP32A
RPLP1	8.17E-09	0.2559595	1	0.994	0.00025342	8	RPLP1
RANBP1	8.23E-09	0.46892139	0.312	0.062	0.00025543	8	RANBP1
RPSA1	8.24E-09	0.58857945	0.645	0.35	0.00025569	8	RPSA1
DNAJB11	8.67E-09	0.47387905	0.656	0.288	0.00026893	8	DNAJB11
TIMM10	8.67E-09	0.449237	0.355	0.063	0.00026906	8	TIMM10
NDUFA12	9.05E-09	0.56943491	0.398	0.103	0.00028084	8	NDUFA12
HNRNPDL1	9.14E-09	0.52682719	0.538	0.209	0.00028358	8	HNRNPDL1
NUCKS12	9.26E-09	0.56769945	0.495	0.171	0.00028728	8	NUCKS12
LBR	9.33E-09	0.59937239	0.29	0.062	0.00028947	8	LBR
ETF1	1.01E-08	0.54171229	0.376	0.101	0.00031191	8	ETF1
NDUFS6	1.03E-08	0.60992195	0.462	0.134	0.00031916	8	NDUFS6
PSMB8	1.04E-08	0.62230702	0.505	0.163	0.00032125	8	PSMB8
LRR1	1.08E-08	0.4263247	0.215	0.019	0.00033591	8	LRR1
SLC25A4	1.08E-08	0.48881069	0.473	0.158	0.00033616	8	SLC25A4
PMPCB	1.08E-08	0.51919381	0.301	0.061	0.00033629	8	PMPCB
ALDOA	1.15E-08	0.5549964	0.656	0.331	0.00035809	8	ALDOA
C19orf53	1.16E-08	0.41441875	0.516	0.181	0.00035848	8	C19orf53
GMNN	1.18E-08	0.42733859	0.247	0.033	0.00036477	8	GMNN
SLIRP	1.20E-08	0.47010172	0.538	0.215	0.00037219	8	SLIRP
APOBEC3C	1.22E-08	0.61883201	0.376	0.103	0.00037884	8	APOBEC3C
GTF3C6	1.27E-08	0.51926168	0.387	0.084	0.00039353	8	GTF3C6
SPCS33	1.42E-08	0.40162369	0.946	0.782	0.00044142	8	SPCS33
SIVA1	1.43E-08	0.47035754	0.548	0.191	0.00044436	8	SIVA1
CCDC167	1.46E-08	0.53030619	0.441	0.133	0.00045417	8	CCDC167
RPSAP58	1.48E-08	0.57626313	0.484	0.154	0.00045915	8	RPSAP58
RPL7A	1.51E-08	0.45939602	0.903	0.678	0.00046833	8	RPL7A
ECT2	1.60E-08	0.43522125	0.151	0.008	0.00049553	8	ECT2
PKM1	1.64E-08	0.47967	0.495	0.169	0.00050919	8	PKM1
TMA72	1.67E-08	0.51883027	0.57	0.241	0.00051726	8	TMA72
CANX1	1.80E-08	0.37719748	0.882	0.552	0.00055929	8	CANX1
RHOA	1.83E-08	0.48529714	0.656	0.31	0.00056908	8	RHOA
MYBL2	1.95E-08	0.39873289	0.151	0.012	0.00060396	8	MYBL2
HBD	1.96E-08	0.65909267	0.204	0.03	0.00060875	8	HBD
DEPDC1	1.98E-08	0.33839566	0.108	0.001	0.00061578	8	DEPDC1
GTSE1	2.07E-08	0.28255334	0.108	0.002	0.00064141	8	GTSE1
PRDX1	2.28E-08	0.44614197	0.753	0.383	0.00070666	8	PRDX1

ILF2	2.46E-08	0.54147447	0.419	0.133	0.0007627	8	ILF2
CCNB1	2.52E-08	0.5430904	0.129	0.006	0.00078237	8	CCNB1
CENPH	2.55E-08	0.44604762	0.129	0.006	0.00079153	8	CENPH
NDUFB7	2.67E-08	0.46621467	0.699	0.331	0.00082766	8	NDUFB7
DAD1	2.71E-08	0.4469995	0.763	0.398	0.00084162	8	DAD1
NDUFB2	2.74E-08	0.43924758	0.645	0.263	0.00084962	8	NDUFB2
NASP	2.75E-08	0.53649021	0.301	0.067	0.00085222	8	NASP
ZWILCH	2.86E-08	0.42496566	0.14	0.013	0.00088731	8	ZWILCH
SRM	2.92E-08	0.43565241	0.29	0.056	0.00090503	8	SRM
STK17B	2.92E-08	0.47506548	0.559	0.21	0.00090648	8	STK17B
MRTO4	2.93E-08	0.52513804	0.247	0.036	0.00090989	8	MRTO4
DCPS	3.17E-08	0.50357965	0.312	0.061	0.00098405	8	DCPS
HSP90AB11	3.27E-08	0.57595915	0.731	0.388	0.001014	8	HSP90AB11
PARK7	3.29E-08	0.55330225	0.57	0.24	0.00101992	8	PARK7
SRSF1	3.30E-08	0.504801	0.344	0.061	0.00102315	8	SRSF1
MRPL1	3.68E-08	0.48719439	0.215	0.03	0.00114348	8	MRPL1
BST2	3.69E-08	0.49892401	0.516	0.166	0.00114574	8	BST2
HBS1L	3.71E-08	0.47866364	0.312	0.064	0.00115204	8	HBS1L
PPP1CA1	3.81E-08	0.54898192	0.462	0.155	0.00118083	8	PPP1CA1
RPA3	4.15E-08	0.54070125	0.323	0.065	0.00128652	8	RPA3
NDUFB111	4.29E-08	0.41712552	0.688	0.325	0.00133245	8	NDUFB111
CHAF1A	4.34E-08	0.29551879	0.108	0.004	0.00134787	8	CHAF1A
SNRPD3	4.71E-08	0.46303924	0.409	0.101	0.00146098	8	SNRPD3
RPLP2	4.80E-08	0.34246822	0.978	0.904	0.00148819	8	RPLP2
NHP2	4.93E-08	0.41684835	0.376	0.104	0.00152933	8	NHP2
FAM136A	5.04E-08	0.52944137	0.387	0.09	0.00156516	8	FAM136A
EXOSC8	5.30E-08	0.43157401	0.312	0.071	0.0016445	8	EXOSC8
SRP19	5.30E-08	0.48866568	0.43	0.106	0.00164604	8	SRP19
MCM5	5.45E-08	0.49821116	0.215	0.02	0.00169136	8	MCM5
NDUFA2	5.47E-08	0.45497104	0.495	0.186	0.00169848	8	NDUFA2
HSPA9	5.64E-08	0.53087968	0.43	0.13	0.0017487	8	HSPA9
RBMX	5.65E-08	0.5845597	0.419	0.129	0.00175321	8	RBMX
ADAM19	5.78E-08	0.38871925	0.28	0.043	0.00179496	8	ADAM19
MRPL11	5.82E-08	0.56381025	0.247	0.046	0.00180486	8	MRPL11
ZNF90	5.93E-08	0.43145407	0.473	0.158	0.0018401	8	ZNF90
GNB2L1	5.98E-08	0.40754762	0.914	0.693	0.00185466	8	GNB2L1
GARS	5.98E-08	0.52656458	0.462	0.146	0.00185504	8	GARS
TFDP1	6.39E-08	0.37442528	0.172	0.011	0.00198395	8	TFDP1
ACTR2	6.42E-08	0.43374971	0.559	0.199	0.00199259	8	ACTR2
CNBP	6.51E-08	0.50181575	0.742	0.373	0.00202054	8	CNBP

TMED10	6.54E-08	0.38042937	0.806	0.402	0.00203041	8	TMED10
EIF3G	6.75E-08	0.48593529	0.452	0.132	0.00209401	8	EIF3G
SLC38A5	6.95E-08	0.47866545	0.344	0.082	0.00215697	8	SLC38A5
GMFG	7.01E-08	0.47328835	0.452	0.157	0.00217651	8	GMFG
NAPA	7.07E-08	0.59119217	0.344	0.068	0.0021926	8	NAPA
CCT5	7.15E-08	0.50604599	0.301	0.068	0.00221942	8	CCT5
IPO5	7.81E-08	0.42835453	0.258	0.049	0.00242288	8	IPO5
DNAJC101	7.84E-08	0.52555475	0.462	0.167	0.00243285	8	DNAJC10
NUF2	8.07E-08	0.34777544	0.14	0.004	0.00250464	8	NUF2
PRDX2	8.22E-08	0.46696812	0.548	0.212	0.00255131	8	PRDX2
PSMC3	8.27E-08	0.53357218	0.452	0.129	0.00256674	8	PSMC3
PEBP1	8.33E-08	0.52400368	0.645	0.301	0.00258643	8	PEBP1
GHITM1	8.45E-08	0.47443814	0.538	0.204	0.00262271	8	GHITM
SEC13	8.93E-08	0.49956781	0.505	0.199	0.00276984	8	SEC13
TMED2	8.94E-08	0.48373364	0.72	0.387	0.00277487	8	TMED2
HSD17B10	9.51E-08	0.44345831	0.344	0.077	0.00295258	8	HSD17B10
VDAC1	1.01E-07	0.4603189	0.333	0.076	0.00314303	8	VDAC1
HMGB3	1.02E-07	0.52166095	0.237	0.031	0.00316512	8	HMGB3
UQCC2	1.08E-07	0.53244124	0.419	0.122	0.00334604	8	UQCC2
HIST1H4H	1.14E-07	0.40655987	0.161	0.023	0.00353226	8	HIST1H4H
SLC35B1	1.19E-07	0.48247958	0.473	0.139	0.00369129	8	SLC35B1
COMMD1	1.25E-07	0.55305228	0.312	0.085	0.00388185	8	COMMD1
RPL18A1	1.29E-07	0.42092226	0.806	0.517	0.0039878	8	RPL18A
TOP1	1.35E-07	0.41692182	0.43	0.137	0.00417386	8	TOP1
RAD21	1.36E-07	0.58189956	0.387	0.104	0.00421697	8	RAD21
NDUFA13	1.37E-07	0.42380665	0.602	0.274	0.00425657	8	NDUFA13
TUFM	1.42E-07	0.42074864	0.559	0.232	0.00440271	8	TUFM
RAC21	1.45E-07	0.5881449	0.344	0.097	0.00448716	8	RAC2
GNL3	1.54E-07	0.51684517	0.591	0.245	0.00479257	8	GNL3
MRPL24	1.60E-07	0.51387041	0.312	0.072	0.0049564	8	MRPL24
FH	1.60E-07	0.49474767	0.172	0.035	0.00495787	8	FH
SSB	1.60E-07	0.38023657	0.344	0.092	0.00496854	8	SSB
PSMD14	1.61E-07	0.44216547	0.376	0.086	0.00499094	8	PSMD14
MTHFD2	1.63E-07	0.53155896	0.495	0.173	0.00506069	8	MTHFD2
YEATS4	1.74E-07	0.36073005	0.183	0.028	0.00539648	8	YEATS4
UBL5	1.91E-07	0.44509197	0.731	0.431	0.00592395	8	UBL5
PDAP1	2.02E-07	0.53289092	0.366	0.092	0.00626178	8	PDAP1
RPL121	2.02E-07	0.38766132	0.892	0.664	0.00626303	8	RPL12
VBP1	2.06E-07	0.53056173	0.312	0.088	0.00639482	8	VBP1
CRNKL1	2.10E-07	0.42232474	0.247	0.041	0.00651019	8	CRNKL1

CDC123	2.11E-07	0.464929	0.247	0.053	0.00655544	8	CDC123
USMG5	2.11E-07	0.41647817	0.634	0.291	0.00655585	8	USMG5
CD48	2.15E-07	0.43965384	0.387	0.113	0.00665767	8	CD48
FARSB	2.17E-07	0.38055955	0.183	0.02	0.00673157	8	FARSB
SMC1A	2.17E-07	0.43757062	0.247	0.038	0.00673217	8	SMC1A
BOLA3	2.18E-07	0.41308174	0.28	0.069	0.00676983	8	BOLA3
SSR12	2.20E-07	0.46572423	0.624	0.314	0.00681219	8	SSR1
UAP1	2.21E-07	0.47338863	0.452	0.179	0.00686211	8	UAP1
YARS	2.21E-07	0.50191846	0.344	0.098	0.00686994	8	YARS
RAD23A1	2.28E-07	0.45372903	0.387	0.119	0.00706199	8	RAD23A
NUP93	2.32E-07	0.26624734	0.108	0.01	0.00721207	8	NUP93
RAD18	2.47E-07	0.37037882	0.108	0.01	0.00765337	8	RAD18
FTH11	2.57E-07	0.31899301	0.849	0.512	0.00798057	8	FTH1
NOLC1	2.66E-07	0.48323111	0.366	0.083	0.00826277	8	NOLC1
ADRM1	2.92E-07	0.46679131	0.366	0.084	0.00905786	8	ADRM1
OAZ1	2.97E-07	0.36268706	0.892	0.648	0.00921864	8	OAZ1
BUB3	2.98E-07	0.52741775	0.323	0.107	0.00925746	8	BUB3
NDUFB10	3.03E-07	0.49528869	0.548	0.23	0.00939095	8	NDUFB10
RPL34	3.07E-07	0.27769313	1	0.883	0.00952479	8	RPL34
LSM6	3.08E-07	0.36140368	0.258	0.06	0.00955887	8	LSM6
MRPS18C	3.12E-07	0.49125471	0.366	0.095	0.00969609	8	MRPS18C
HIST1H2BJ	3.15E-07	0.31786255	0.151	0.016	0.00977358	8	HIST1H2BJ
DNAJC9	3.19E-07	0.51943473	0.204	0.034	0.00989373	8	DNAJC9
NDUFA3	3.22E-07	0.55162295	0.57	0.252	0.01000152	8	NDUFA3
NHP2L11	3.24E-07	0.50450315	0.527	0.229	0.01004213	8	NHP2L1
SRSF2	3.24E-07	0.46109181	0.505	0.202	0.01005317	8	SRSF2
EIF4G2	3.49E-07	0.44725605	0.624	0.303	0.01083378	8	EIF4G2
SEPT11	3.58E-07	0.37136057	0.237	0.042	0.01109994	8	SEPT11
EIF1AX	3.67E-07	0.48627376	0.43	0.131	0.0113799	8	EIF1AX
PHF19	3.71E-07	0.37073237	0.151	0.012	0.01151836	8	PHF19
CLEC2B1	3.92E-07	0.67827684	0.333	0.096	0.01217507	8	CLEC2B
SNHG5	4.02E-07	0.43860444	0.828	0.522	0.01247258	8	SNHG5
NDUFB3	4.22E-07	0.41920788	0.484	0.16	0.01309479	8	NDUFB3
HELLS	4.22E-07	0.3537419	0.161	0.013	0.01310018	8	HELLS
SSSCA1	4.32E-07	0.52041697	0.28	0.067	0.01340809	8	SSSCA1
NDUFC2	4.44E-07	0.48394274	0.538	0.238	0.01377602	8	NDUFC2
UBB2	4.44E-07	0.39331753	0.935	0.776	0.01378527	8	UBB
CAP1	4.54E-07	0.44830738	0.484	0.177	0.01410335	8	CAP1
NDUFAF2	4.66E-07	0.38109873	0.237	0.034	0.0144523	8	NDUFAF2
TXNL1	4.77E-07	0.51263856	0.409	0.125	0.01480992	8	TXNL1

EMC7	4.92E-07	0.40870364	0.398	0.129	0.01527795	8	EMC7
SLBP	5.25E-07	0.57165185	0.237	0.05	0.01629062	8	SLBP
CALU	5.43E-07	0.51411251	0.57	0.233	0.01683954	8	CALU
PPIH	5.54E-07	0.29947345	0.151	0.014	0.01718053	8	PPIH
MRPL47	5.57E-07	0.42232426	0.237	0.055	0.01728739	8	MRPL47
GSTP11	5.58E-07	0.36976544	0.871	0.594	0.01731074	8	GSTP1
NOL7	5.78E-07	0.54915083	0.548	0.238	0.01792895	8	NOL7
CCT3	5.86E-07	0.43722174	0.323	0.083	0.01818273	8	CCT3
PAFAH1B3	6.07E-07	0.44887953	0.183	0.028	0.01884878	8	PAFAH1B3
HLA-A	6.13E-07	0.51269005	0.796	0.494	0.01903318	8	HLA-A
EIF3H	6.27E-07	0.41570033	0.505	0.18	0.01944485	8	EIF3H
GPX12	6.59E-07	0.45236424	0.516	0.225	0.02046033	8	GPX1
OXCT1	6.82E-07	0.32177378	0.183	0.023	0.02117491	8	OXCT1
ZNF593	6.87E-07	0.5646801	0.366	0.085	0.02133021	8	ZNF593
EZH2	7.06E-07	0.42332053	0.226	0.03	0.02191503	8	EZH2
DERL1	7.48E-07	0.39252158	0.516	0.202	0.0232243	8	DERL1
LSM5	7.71E-07	0.52899955	0.473	0.163	0.0239147	8	LSM5
COX7C	8.51E-07	0.41708338	0.806	0.543	0.02642138	8	COX7C
PCMT1	8.65E-07	0.37520909	0.366	0.107	0.02682984	8	PCMT1
EIF2S2	8.99E-07	0.43800929	0.495	0.177	0.02789511	8	EIF2S2
NIPA2	9.11E-07	0.39446086	0.344	0.087	0.02825984	8	NIPA2
YWHAB	9.21E-07	0.51425004	0.527	0.213	0.02857357	8	YWHAB
GTF2A2	9.23E-07	0.50491278	0.323	0.096	0.02862883	8	GTF2A2
TRMT10C	9.35E-07	0.45644889	0.215	0.045	0.02900838	8	TRMT10C
CHEK1	9.36E-07	0.31730159	0.14	0.006	0.02904335	8	CHEK1
RWDD1	9.37E-07	0.39696723	0.452	0.142	0.02909111	8	RWDD1
SNHG6	9.66E-07	0.4405186	0.462	0.179	0.02998283	8	SNHG6
CHCHD3	9.72E-07	0.42994968	0.29	0.06	0.03016136	8	CHCHD3
ARF1	9.99E-07	0.36650672	0.71	0.355	0.03100884	8	ARF1
ATPIF1	1.01E-06	0.38375588	0.667	0.337	0.03121383	8	ATPIF1
C8orf59	1.01E-06	0.47234656	0.602	0.251	0.03142018	8	C8orf59
LSM2	1.02E-06	0.46495461	0.312	0.076	0.03177319	8	LSM2
STOML2	1.06E-06	0.52556595	0.333	0.097	0.03283868	8	STOML2
MRPL14	1.07E-06	0.45171774	0.323	0.085	0.03323272	8	MRPL14
EWSR11	1.09E-06	0.47770914	0.366	0.12	0.03381926	8	EWSR1
DLEU2	1.09E-06	0.35487132	0.194	0.015	0.03391665	8	DLEU2
GAR1	1.11E-06	0.43448858	0.151	0.025	0.03432503	8	GAR1
PCNA	1.12E-06	0.62640684	0.194	0.033	0.03490368	8	PCNA
TOMM22	1.18E-06	0.49130338	0.312	0.07	0.03657654	8	TOMM22
RPS20	1.20E-06	0.31712112	0.946	0.812	0.03720989	8	RPS20

NONO	1.23E-06	0.40506897	0.312	0.085	0.03822559	8	NONO
PSMD11	1.24E-06	0.42595445	0.301	0.067	0.03852329	8	PSMD11
YIF1B	1.34E-06	0.3608068	0.237	0.04	0.04163945	8	YIF1B
CCT8	1.34E-06	0.40013461	0.452	0.144	0.04168293	8	CCT8
MRPL13	1.44E-06	0.46269567	0.29	0.065	0.04457293	8	MRPL13
HCST	1.44E-06	0.46282479	0.226	0.049	0.04461142	8	HCST
ANAPC5	1.44E-06	0.41071244	0.57	0.246	0.044783	8	ANAPC5
PTGES3	1.45E-06	0.45819334	0.452	0.161	0.04487687	8	PTGES3
UQCRCFS1	1.49E-06	0.49634884	0.366	0.111	0.04628005	8	UQCRCFS1
NUP210	1.50E-06	0.39143045	0.172	0.026	0.0466306	8	NUP210
RER1	1.51E-06	0.41726907	0.505	0.192	0.04692918	8	RER1
PFDN6	1.53E-06	0.39002687	0.28	0.06	0.0473679	8	PFDN6
RPL7L1	1.53E-06	0.50843488	0.258	0.063	0.04762991	8	RPL7L1
ILF3	1.56E-06	0.42375455	0.376	0.113	0.04829196	8	ILF3
FDPS	1.56E-06	0.41126688	0.409	0.148	0.04829871	8	FDPS
DDX1	1.58E-06	0.49387399	0.376	0.116	0.04910609	8	DDX1

Supplemental Table E2. Patient-specific genes.

	p_val	avg_logFC	pct.1	pct.2	p_val_adj	cluster	gene
STATH	1.34E-261	3.17940296	0.925	0.084	4.14E-257	1 CRSsNP	STATH
LYZ	2.17E-100	1.79753982	0.62	0.086	6.74E-96	1 CRSsNP	LYZ
ZG16B	8.66E-86	1.32566813	0.442	0.025	2.69E-81	1 CRSsNP	ZG16B
BPIFA1	2.22E-74	1.35462889	0.822	0.353	6.90E-70	1 CRSsNP	BPIFA1
LTF	5.23E-52	1.05115302	0.315	0.023	1.62E-47	1 CRSsNP	LTF
C6orf58	4.93E-49	0.77152993	0.202	0.002	1.53E-44	1 CRSsNP	C6orf58
MSMB	4.59E-43	0.80940985	0.332	0.039	1.42E-38	1 CRSsNP	MSMB
KLF6	5.34E-39	0.98268568	0.822	0.527	1.66E-34	1 CRSsNP	KLF6
JUN	8.38E-39	0.84109077	0.932	0.737	2.60E-34	1 CRSsNP	JUN
BPIFB1	1.60E-33	0.85963072	0.627	0.269	4.95E-29	1 CRSsNP	BPIFB1
SCGB3A1	3.13E-32	0.53394647	0.161	0.006	9.73E-28	1 CRSsNP	SCGB3A1
PIP	1.11E-29	0.53718511	0.134	0.002	3.44E-25	1 CRSsNP	PIP
TNFAIP3	2.16E-27	0.88893271	0.514	0.218	6.71E-23	1 CRSsNP	TNFAIP3
CCL3	3.11E-27	1.79934558	0.291	0.088	9.66E-23	1 CRSsNP	CCL3
SLPI	3.64E-27	0.68731741	0.815	0.525	1.13E-22	1 CRSsNP	SLPI
AZGP1	1.69E-26	0.57548379	0.147	0.007	5.24E-22	1 CRSsNP	AZGP1
NFKBIA	4.92E-26	0.66547316	0.846	0.608	1.53E-21	1 CRSsNP	NFKBIA
IGKC	3.23E-22	1.43465858	0.716	0.682	1.00E-17	1 CRSsNP	IGKC
SRGN	2.06E-21	0.63110496	0.87	0.66	6.41E-17	1 CRSsNP	SRGN
MUC5B	2.14E-21	0.89000583	0.12	0.007	6.63E-17	1 CRSsNP	MUC5B
SCGB1A1	8.24E-21	0.52192407	0.171	0.023	2.56E-16	1 CRSsNP	SCGB1A1
PPP1R15A	7.54E-20	0.55401178	0.764	0.509	2.34E-15	1 CRSsNP	PPP1R15A
IER2	1.35E-19	0.6313212	0.592	0.337	4.18E-15	1 CRSsNP	IER2
PIGR	3.04E-19	0.63649797	0.329	0.1	9.44E-15	1 CRSsNP	PIGR
RP11-1143G9.4	2.41E-17	0.44847554	0.106	0.008	7.48E-13	1 CRSsNP	RP11-1143G9.4
CD79A	4.11E-17	0.54386144	0.682	0.449	1.27E-12	1 CRSsNP	CD79A
FOSB	1.41E-16	0.48814206	0.753	0.516	4.38E-12	1 CRSsNP	FOSB
BIRC3	1.79E-16	0.60850561	0.507	0.24	5.57E-12	1 CRSsNP	BIRC3
ODAM	1.82E-15	0.38214715	0.116	0.016	5.64E-11	1 CRSsNP	ODAM
CCL4	2.61E-15	1.43330181	0.229	0.102	8.11E-11	1 CRSsNP	CCL4
FDCSP	7.60E-15	0.68151966	0.154	0.029	2.36E-10	1 CRSsNP	FDCSP
IL2RG	3.59E-14	0.4593808	0.305	0.111	1.11E-09	1 CRSsNP	IL2RG
DMBT1	5.80E-14	0.32264844	0.103	0.01	1.80E-09	1 CRSsNP	DMBT1
PPDPF	9.43E-14	0.44866155	0.318	0.132	2.93E-09	1 CRSsNP	PPDPF
ISCU	1.69E-13	0.43919062	0.49	0.252	5.25E-09	1 CRSsNP	ISCU
NUCB2	4.75E-13	0.44424941	0.651	0.417	1.47E-08	1 CRSsNP	NUCB2
TXNIP	5.97E-13	0.47238838	0.603	0.362	1.85E-08	1 CRSsNP	TXNIP

EGR1	6.71E-13	0.47902715	0.558	0.345	2.08E-08	1_CRSsNP	EGR1
TNFRSF17	8.78E-13	0.46737282	0.534	0.316	2.72E-08	1_CRSsNP	TNFRSF17
RGS1	1.61E-12	0.49144758	0.812	0.671	4.98E-08	1_CRSsNP	RGS1
CTHRC1	1.87E-12	0.34820952	0.134	0.025	5.79E-08	1_CRSsNP	CTHRC1
MIR155HG	2.58E-12	0.39613937	0.182	0.048	8.00E-08	1_CRSsNP	MIR155HG
RPL30	5.03E-12	0.34087118	0.952	0.856	1.56E-07	1_CRSsNP	RPL30
PELI1	5.55E-12	0.54390464	0.298	0.136	1.72E-07	1_CRSsNP	PELI1
EAF2	1.05E-11	0.44619616	0.527	0.291	3.26E-07	1_CRSsNP	EAF2
RASGRP3	2.02E-11	0.40597738	0.168	0.044	6.28E-07	1_CRSsNP	RASGRP3
MOXD1	2.48E-11	0.40292495	0.144	0.032	7.69E-07	1_CRSsNP	MOXD1
CD74	4.22E-11	0.34884604	0.795	0.631	1.31E-06	1_CRSsNP	CD74
VIM	7.37E-11	0.40093297	0.719	0.541	2.29E-06	1_CRSsNP	VIM
LMO4	7.50E-11	0.44390811	0.305	0.13	2.33E-06	1_CRSsNP	LMO4
EZR	1.62E-10	0.45867265	0.555	0.366	5.02E-06	1_CRSsNP	EZR
PSAP	1.64E-10	0.31752543	0.753	0.553	5.10E-06	1_CRSsNP	PSAP
HLA-E	3.56E-10	0.28735355	0.788	0.605	1.10E-05	1_CRSsNP	HLA-E
LMNA	1.94E-09	0.44768399	0.363	0.2	6.02E-05	1_CRSsNP	LMNA
GPR160	3.02E-09	0.33043652	0.247	0.099	9.38E-05	1_CRSsNP	GPR160
TNFRSF13B	4.13E-09	0.27892625	0.11	0.028	0.00012823	1_CRSsNP	TNFRSF13B
HSH2D	7.62E-09	0.35562807	0.281	0.122	0.00023654	1_CRSsNP	HSH2D
CDC42SE2	1.05E-08	0.35596138	0.291	0.138	0.00032676	1_CRSsNP	CDC42SE2
MT-ND2	1.64E-08	0.28677421	0.575	0.363	0.00050849	1_CRSsNP	MT-ND2
DUSP1	3.29E-08	0.44262878	0.729	0.591	0.0010201	1_CRSsNP	DUSP1
PDCD4	3.39E-08	0.29417377	0.315	0.159	0.00105335	1_CRSsNP	PDCD4
ZFP36	4.40E-08	0.29514794	0.712	0.538	0.00136499	1_CRSsNP	ZFP36
RPLP2	6.69E-08	0.27770006	0.955	0.899	0.0020751	1_CRSsNP	RPLP2
ITM2B	7.38E-08	0.27757424	0.562	0.354	0.00229167	1_CRSsNP	ITM2B
JUNB	1.32E-07	0.26673458	0.692	0.514	0.0040924	1_CRSsNP	JUNB
SERPINB9	1.38E-07	0.30306355	0.144	0.048	0.00429469	1_CRSsNP	SERPINB9
CCL5	3.46E-07	0.48902021	0.13	0.048	0.01073156	1_CRSsNP	CCL5
BTN3A2	4.51E-07	0.25912836	0.188	0.077	0.01400252	1_CRSsNP	BTN3A2
AC104024.1	4.96E-07	0.30544633	0.11	0.027	0.01539117	1_CRSsNP	AC104024.1
SERINC1	6.70E-07	0.28365594	0.226	0.106	0.02080156	1_CRSsNP	SERINC1
IGKJ3	6.89E-07	0.93219925	0.161	0.078	0.02139549	1_CRSsNP	IGKJ3
LINC00657	1.02E-06	0.29729166	0.305	0.171	0.03178561	1_CRSsNP	LINC00657
TMEM205	1.29E-06	0.28515966	0.305	0.16	0.04001016	1_CRSsNP	TMEM205
IGKC1	2.94E-40	0.9666832	0.766	0.644	9.13E-36	2_CRSwNP	IGKC
IGHA1	5.45E-31	0.57219361	0.93	0.954	1.69E-26	2_CRSwNP	IGHA1
IGHM	1.54E-27	1.17893088	0.49	0.25	4.79E-23	2_CRSwNP	IGHM
IGKV1-271	5.94E-27	1.79706538	0.185	0.057	1.84E-22	2_CRSwNP	IGKV1-271

TTC26	1.48E-23	0.56006347	0.202	0.059	4.60E-19	2_CRSwNP	TTC26
MZB1	1.30E-15	0.2877454	0.937	0.9	4.04E-11	2_CRSwNP	MZB1
IGHA2	3.23E-15	0.31806722	0.8	0.717	1.00E-10	2_CRSwNP	IGHA2
SIK1	1.05E-14	0.42111446	0.543	0.395	3.25E-10	2_CRSwNP	SIK1
RPS28	5.00E-13	0.37551306	0.574	0.456	1.55E-08	2_CRSwNP	RPS28
PPIB	9.47E-10	0.34371236	0.685	0.627	2.94E-05	2_CRSwNP	PPIB
RAB30	2.20E-09	0.46604677	0.328	0.23	6.82E-05	2_CRSwNP	RAB30
ITM2C	6.05E-09	0.31526478	0.609	0.512	0.00018766	2_CRSwNP	ITM2C
XBP11	6.68E-09	0.27577358	0.83	0.793	0.00020739	2_CRSwNP	XBP11
SNHG9	1.14E-08	0.34547233	0.197	0.107	0.00035368	2_CRSwNP	SNHG9
CALR	1.36E-08	0.32759167	0.592	0.512	0.00042314	2_CRSwNP	CALR
MAPKAPK21	3.02E-08	0.38455299	0.22	0.131	0.00093842	2_CRSwNP	MAPKAPK2
YPEL5	3.59E-08	0.36812661	0.511	0.413	0.00111506	2_CRSwNP	YPEL5
FKBP111	4.31E-08	0.25253005	0.717	0.647	0.0013375	2_CRSwNP	FKBP11
RGS2	4.65E-08	0.43318367	0.335	0.234	0.00144436	2_CRSwNP	RGS2
RBM3	5.82E-08	0.34161703	0.456	0.362	0.00180589	2_CRSwNP	RBM3
AL928768.3	8.70E-08	0.54141638	0.215	0.132	0.00269844	2_CRSwNP	AL928768.3
SEC61G	1.09E-07	0.30426432	0.508	0.421	0.00339073	2_CRSwNP	SEC61G
TPD52	1.84E-07	0.31270168	0.397	0.299	0.00570937	2_CRSwNP	TPD52
VIMP	1.98E-07	0.28388463	0.629	0.555	0.00614024	2_CRSwNP	VIMP
SNHG8	2.01E-07	0.59751728	0.342	0.259	0.00623144	2_CRSwNP	SNHG8
LY9	2.37E-07	0.36388786	0.144	0.079	0.00736669	2_CRSwNP	LY9
TRMT112	3.14E-07	0.29630839	0.386	0.292	0.00974721	2_CRSwNP	TRMT112
RGS11	3.15E-07	0.31014416	0.734	0.665	0.00978598	2_CRSwNP	RGS1
TNFRSF171	7.21E-07	0.36214988	0.403	0.313	0.02235953	2_CRSwNP	TNFRSF17
IGHG42	3.37E-215	2.09139312	0.896	0.361	1.05E-210	3_AERD	IGHG4
IGHG22	7.42E-84	0.7030275	0.725	0.355	2.30E-79	3_AERD	IGHG2
IGKV3-202	2.87E-77	1.2781926	0.457	0.126	8.91E-73	3_AERD	IGKV3-20
IGKV3OR2-2682	1.68E-58	1.48360679	0.226	0.027	5.20E-54	3_AERD	IGKV3OR2-268
IGHV3-212	2.34E-54	2.10064101	0.333	0.085	7.27E-50	3_AERD	IGHV3-21
IGHG11	5.98E-51	0.3533066	0.822	0.513	1.86E-46	3_AERD	IGHG1
IGKV3D-202	4.87E-43	0.84838391	0.288	0.078	1.51E-38	3_AERD	IGKV3D-20
MTRNR2L121	1.78E-42	0.59827123	0.703	0.449	5.53E-38	3_AERD	MTRNR2L12
CCND21	5.47E-40	0.58764402	0.561	0.296	1.70E-35	3_AERD	CCND2
IGHE1	4.10E-39	0.82825709	0.147	0.012	1.27E-34	3_AERD	IGHE
POSTN2	5.71E-36	0.61022648	0.479	0.241	1.77E-31	3_AERD	POSTN
FBRSL1	2.89E-32	0.90338937	0.119	0.01	8.96E-28	3_AERD	FBRSL1
RPL102	3.16E-32	0.45478888	0.778	0.6	9.81E-28	3_AERD	RPL10
SERPINB32	1.42E-30	0.64723581	0.384	0.184	4.41E-26	3_AERD	SERPINB3

IGHV4-392	2.99E-27	0.80979889	0.255	0.091	9.28E-23	3_AERD	IGHV4-39
RPS3A2	7.30E-27	0.50590012	0.551	0.367	2.27E-22	3_AERD	RPS3A
IGHV1-82	1.39E-26	1.32487259	0.184	0.051	4.30E-22	3_AERD	IGHV1-8
IL5RA2	5.10E-26	0.61118684	0.236	0.095	1.58E-21	3_AERD	IL5RA
KREMEN11	5.33E-26	0.64200403	0.123	0.022	1.65E-21	3_AERD	KREMEN1
RPL13A1	2.80E-23	0.30586138	0.909	0.812	8.67E-19	3_AERD	RPL13A
RPL362	3.86E-23	0.38594329	0.718	0.56	1.20E-18	3_AERD	RPL36
ANXA12	1.24E-21	0.41657538	0.487	0.321	3.84E-17	3_AERD	ANXA1
RPL411	1.90E-21	0.2577014	0.917	0.83	5.91E-17	3_AERD	RPL41
IGHV1-182	3.85E-21	1.40601936	0.253	0.116	1.20E-16	3_AERD	IGHV1-18
RPS271	1.67E-20	0.40918108	0.638	0.48	5.20E-16	3_AERD	RPS27
IGKV3D-7	8.83E-20	0.51591403	0.11	0.023	2.74E-15	3_AERD	IGKV3D-7
BNIP31	1.10E-19	1.1034425	0.137	0.047	3.40E-15	3_AERD	BNIP3
RPL18A2	2.78E-19	0.45028589	0.595	0.449	8.62E-15	3_AERD	RPL18A
MTRNR2L14	2.62E-18	0.25807264	0.81	0.673	8.14E-14	3_AERD	MTRNR2L1
CLC	6.21E-18	0.32035248	0.133	0.04	1.93E-13	3_AERD	CLC
IGLC21	1.80E-17	0.78409086	0.348	0.21	5.58E-13	3_AERD	IGLC2
IGHV3-482	4.49E-17	0.95822329	0.222	0.1	1.39E-12	3_AERD	IGHV3-48
RPL172	7.74E-17	0.53105055	0.353	0.241	2.40E-12	3_AERD	RPL17
IGKV3D-112	1.24E-16	1.02056085	0.173	0.066	3.84E-12	3_AERD	IGKV3D-11
MTRNR2L81	2.11E-16	0.31411442	0.748	0.597	6.54E-12	3_AERD	MTRNR2L8
RPL91	1.01E-15	0.39373944	0.57	0.434	3.15E-11	3_AERD	RPL9
IGKJ51	6.67E-15	1.44548597	0.208	0.111	2.07E-10	3_AERD	IGKJ5
CD91	8.04E-15	0.40921521	0.34	0.212	2.50E-10	3_AERD	CD9
RPL3	9.57E-15	0.28097552	0.891	0.825	2.97E-10	3_AERD	RPL3
IGKV3-71	2.62E-13	0.47798197	0.182	0.084	8.12E-09	3_AERD	IGKV3-7
AC096579.72	1.63E-12	0.5390376	0.628	0.498	5.06E-08	3_AERD	AC096579.7
RPL72	3.51E-12	0.43787159	0.204	0.118	1.09E-07	3_AERD	RPL7
IGKV3-111	4.67E-12	0.40371385	0.256	0.124	1.45E-07	3_AERD	IGKV3-11
IGHV1-21	4.73E-12	0.92364185	0.148	0.064	1.47E-07	3_AERD	IGHV1-2
IGHV1-242	1.34E-11	0.98599445	0.297	0.154	4.14E-07	3_AERD	IGHV1-24
ALOX151	6.22E-11	0.3595613	0.179	0.097	1.93E-06	3_AERD	ALOX15
MTRNR2L31	1.30E-10	0.29867829	0.405	0.292	4.03E-06	3_AERD	MTRNR2L3
MIF1	5.87E-10	0.31114577	0.495	0.395	1.82E-05	3_AERD	MIF
GUSBP111	8.16E-10	1.04932362	0.297	0.222	2.53E-05	3_AERD	GUSBP11
RPL291	9.02E-10	0.27518113	0.503	0.393	2.80E-05	3_AERD	RPL29
IGHV3-642	3.24E-09	0.89978463	0.148	0.077	0.00010056	3_AERD	IGHV3-64
TACSTD21	9.48E-09	0.29052341	0.233	0.145	0.00029429	3_AERD	TACSTD2
CST11	2.63E-08	0.27626045	0.179	0.101	0.00081463	3_AERD	CST1
VMO1	3.64E-08	0.26835889	0.165	0.096	0.00112835	3_AERD	VMO1

IGHV6-1	5.04E-08	0.25254356	0.109	0.051	0.00156474	3_AERD	IGHV6-1
YBX11	5.69E-08	0.31169893	0.346	0.259	0.00176524	3_AERD	YBX11
HIST1H4C1	9.78E-08	0.34348674	0.289	0.204	0.00303554	3_AERD	HIST1H4C
RPL22	2.25E-07	0.29097498	0.304	0.222	0.00697038	3_AERD	RPL22
PLD31	2.28E-07	0.30166643	0.207	0.148	0.00706428	3_AERD	PLD3
S100A21	4.74E-07	0.25749328	0.268	0.188	0.0147178	3_AERD	S100A2
CEP128	1.05E-06	0.29531781	0.15	0.097	0.03262812	3_AERD	CEP128

References

1. Bhattacharyya N. Influence of polyps on outcomes after endoscopic sinus surgery. *The Laryngoscope*. 2007;117(10):1834-1838.
2. Smith KA, Orlandi RR, Rudmik L. Cost of adult chronic rhinosinusitis: A systematic review. *The Laryngoscope*. 2015;125(7):1547-1556.
3. Bhattacharyya N. Assessing the additional disease burden of polyps in chronic rhinosinusitis. *The Annals of otology, rhinology, and laryngology*. 2009;118(3):185-189.
4. Bochenek G, Nagraba K, Nizankowska E, Szczechlik A. A controlled study of 9alpha,11beta-PGF2 (a prostaglandin D2 metabolite) in plasma and urine of patients with bronchial asthma and healthy controls after aspirin challenge. *The Journal of allergy and clinical immunology*. 2003;111(4):743-749.
5. Cahill KN, Bensko JC, Boyce JA, Laidlaw TM. Prostaglandin D(2): a dominant mediator of aspirin-exacerbated respiratory disease. *The Journal of allergy and clinical immunology*. 2015;135(1):245-252.
6. Buchheit KM, Cahill KN, Katz HR, et al. Thymic stromal lymphopoietin controls prostaglandin D2 generation in patients with aspirin-exacerbated respiratory disease. *The Journal of allergy and clinical immunology*. 2016;137(5):1566-1576 e1565.
7. McMains KC, Kountakis SE. Medical and surgical considerations in patients with Samter's triad. *American journal of rhinology*. 2006;20(6):573-576.
8. Tan BK, Li QZ, Suh L, et al. Evidence for intranasal antinuclear autoantibodies in patients with chronic rhinosinusitis with nasal polyps. *The Journal of allergy and clinical immunology*. 2011;128(6):1198-1206 e1191.
9. Peters AT, Kato A, Zhang N, et al. Evidence for altered activity of the IL-6 pathway in chronic rhinosinusitis with nasal polyps. *The Journal of allergy and clinical immunology*. 2010;125(2):397-403 e310.
10. Van Zele T, Gevaert P, Holtappels G, van Cauwenberge P, Bachert C. Local immunoglobulin production in nasal polyposis is modulated by superantigens. *Clinical and experimental allergy : journal of the British Society for Allergy and Clinical Immunology*. 2007;37(12):1840-1847.
11. Hulse KE, Norton JE, Suh L, et al. Chronic rhinosinusitis with nasal polyps is characterized by B-cell inflammation and EBV-induced protein 2 expression. *The Journal of allergy and clinical immunology*. 2013;131(4):1075-1083, 1083 e1071-1077.
12. Groot Kormelink T, Calus L, De Ruyck N, et al. Local free light chain expression is increased in chronic rhinosinusitis with nasal polyps. *Allergy*. 2012;67(9):1165-1172.
13. Bartemes KR, Cooper KM, Drain KL, Kita H. Secretory IgA induces antigen-independent eosinophil survival and cytokine production without inducing effector functions. *The Journal of allergy and clinical immunology*. 2005;116(4):827-835.
14. Van Zele T, Coppieters F, Gevaert P, Holtappels G, Van Cauwenberge P, Bachert C. Local complement activation in nasal polyposis. *Laryngoscope*. 2009;119(9):1753-1758.
15. Gevaert P, Holtappels G, Johansson SG, Cuvelier C, Cauwenberge P, Bachert C. Organization of secondary lymphoid tissue and local IgE formation to *Staphylococcus aureus* enterotoxins in nasal polyp tissue. *Allergy*. 2005;60(1):71-79.
16. Bachert C, Zhang N, Holtappels G, et al. Presence of IL-5 protein and IgE antibodies to staphylococcal enterotoxins in nasal polyps is associated with comorbid asthma. *The Journal of allergy and clinical immunology*. 2010;126(5):962-968, 968 e961-966.
17. Szczechlik A, Schmitz-Schumann M, Nizankowska E, Milewski M, Roehlig F, Virchow C. Altered distribution of IgG subclasses in aspirin-induced asthma: high IgG4, low IgG1. *Clinical and experimental allergy : journal of the British Society for Allergy and Clinical Immunology*. 1992;22(2):283-287.

18. Koyama T, Kariya S, Sato Y, et al. Significance of IgG4-positive cells in severe eosinophilic chronic rhinosinusitis. *Allergology international : official journal of the Japanese Society of Allergology*. 2018.
19. Hulse KE, Stevens WW, Tan BK, Schleimer RP. Pathogenesis of nasal polyposis. *Clinical and experimental allergy : journal of the British Society for Allergy and Clinical Immunology*. 2015;45(2):328-346.
20. Stevens WW, Ocampo CJ, Berdnikovs S, et al. Cytokines in Chronic Rhinosinusitis. Role in Eosinophilia and Aspirin-exacerbated Respiratory Disease. *American journal of respiratory and critical care medicine*. 2015;192(6):682-694.
21. Liu T, Kanacka Y, Barrett NA, et al. Aspirin-Exacerbated Respiratory Disease Involves a Cysteinyl Leukotriene-Driven IL-33-Mediated Mast Cell Activation Pathway. *Journal of immunology*. 2015;195(8):3537-3545.
22. Hershey GK, Friedrich MF, Esswein LA, Thomas ML, Chatila TA. The association of atopy with a gain-of-function mutation in the alpha subunit of the interleukin-4 receptor. *The New England journal of medicine*. 1997;337(24):1720-1725.
23. Cocks BG, de Waal Malefyt R, Galizzi JP, de Vries JE, Aversa G. IL-13 induces proliferation and differentiation of human B cells activated by the CD40 ligand. *Int Immunol*. 1993;5(6):657-663.
24. Meltzer EO, Hamilos DL, Hadley JA, et al. Rhinosinusitis: establishing definitions for clinical research and patient care. *The Journal of allergy and clinical immunology*. 2004;114(6 Suppl):155-212.
25. Dwyer DF, Barrett NA, Austen KF, Immunological Genome Project C. Expression profiling of constitutive mast cells reveals a unique identity within the immune system. *Nature immunology*. 2016;17(7):878-887.
26. Ordovas-Montanes J, Dwyer DF, Nyquist SK, et al. Allergic inflammatory memory in human respiratory epithelial progenitor cells. *Nature*. 2018;560(7720):649-654.
27. Butler A, Hoffman P, Smibert P, Papalexi E, Satija R. Integrating single-cell transcriptomic data across different conditions, technologies, and species. *Nat Biotechnol*. 2018;36(5):411-420.
28. Trapnell C, Cacchiarelli D, Grimsby J, et al. The dynamics and regulators of cell fate decisions are revealed by pseudotemporal ordering of single cells. *Nat Biotechnol*. 2014;32(4):381-386.
29. Wambre E, Bajzik V, DeLong JH, et al. A phenotypically and functionally distinct human TH2 cell subpopulation is associated with allergic disorders. *Sci Transl Med*. 2017;9(401).
30. Yang Z, Robinson MJ, Allen CD. Regulatory constraints in the generation and differentiation of IgE-expressing B cells. *Curr Opin Immunol*. 2014;28:64-70.
31. Johns CB, Laidlaw TM. Elevated total serum IgE in nonatopic patients with aspirin-exacerbated respiratory disease. *American journal of rhinology & allergy*. 2014;28(4):287-289.
32. Hayashi H, Mitsui C, Nakatani E, et al. Omalizumab reduces cysteinyl leukotriene and 9alpha,11beta-prostaglandin F2 overproduction in aspirin-exacerbated respiratory disease. *The Journal of allergy and clinical immunology*. 2016;137(5):1585-1587 e1584.
33. Jeannin P, Lecoanet S, Delneste Y, Gauchat JF, Bonnefoy JY. IgE versus IgG4 production can be differentially regulated by IL-10. *Journal of immunology*. 1998;160(7):3555-3561.
34. Santos AF, James LK, Bahnsen HT, et al. IgG4 inhibits peanut-induced basophil and mast cell activation in peanut-tolerant children sensitized to peanut major allergens. *The Journal of allergy and clinical immunology*. 2015;135(5):1249-1256.
35. Adjobimey T, Hoerauf A. Induction of immunoglobulin G4 in human filariasis: an indicator of immunoregulation. *Ann Trop Med Parasitol*. 2010;104(6):455-464.

36. Clayton F, Fang JC, Gleich GJ, et al. Eosinophilic esophagitis in adults is associated with IgG4 and not mediated by IgE. *Gastroenterology*. 2014;147(3):602-609.
37. Stone JH, Zen Y, Deshpande V. IgG4-related disease. *The New England journal of medicine*. 2012;366(6):539-551.
38. Takatsu K, Tominaga A, Hamaoka T. Antigen-induced T cell-replacing factor (TRF). I. Functional characterization of a TRF-producing helper T cell subset and genetic studies on TRF production. *Journal of immunology*. 1980;124(5):2414-2422.
39. Takatsu K. Interleukin 5 and B cell differentiation. *Cytokine Growth Factor Rev*. 1998;9(1):25-35.
40. Hitoshi Y, Yamaguchi N, Mita S, et al. Distribution of IL-5 receptor-positive B cells. Expression of IL-5 receptor on Ly-1(CD5)+ B cells. *Journal of immunology*. 1990;144(11):4218-4225.
41. Cassese G, Arce S, Hauser AE, et al. Plasma cell survival is mediated by synergistic effects of cytokines and adhesion-dependent signals. *Journal of immunology*. 2003;171(4):1684-1690.
42. Pene J, Rousset F, Briere F, et al. Interleukin 5 enhances interleukin 4-induced IgE production by normal human B cells. The role of soluble CD23 antigen. *European journal of immunology*. 1988;18(6):929-935.
43. Crestani E, Lohman IC, Guerra S, Wright AL, Halonen M. Association of IL-5 cytokine production and in vivo IgE levels in infants and parents. *The Journal of allergy and clinical immunology*. 2007;120(4):820-826.
44. Haldar P, Brightling CE, Hargadon B, et al. Mepolizumab and exacerbations of refractory eosinophilic asthma. *The New England journal of medicine*. 2009;360(10):973-984.
45. Gevaert P, Van Bruaene N, Cattaert T, et al. Mepolizumab, a humanized anti-IL-5 mAb, as a treatment option for severe nasal polyposis. *The Journal of allergy and clinical immunology*. 2011;128(5):989-995 e981-988.
46. Bachert C, Sousa AR, Lund VJ, et al. Reduced need for surgery in severe nasal polyposis with mepolizumab: Randomized trial. *The Journal of allergy and clinical immunology*. 2017;140(4):1024-1031 e1014.
47. Tuttle KL, Buchheit KM, Laidlaw TM, Cahill KN. A retrospective analysis of mepolizumab in subjects with aspirin-exacerbated respiratory disease. *J Allergy Clin Immunol Pract*. 2018;6(3):1045-1047.
48. Laidlaw TM, Prussin C, Panettieri RA, et al. Dexramipexole depletes blood and tissue eosinophils in nasal polyps with no change in polyp size. *Laryngoscope*. 2018.